Insulin-Mimetic Signaling by the Sulfonylurea Glimepiride and Phosphoinositolglycans Involves Distinct Mechanisms for Redistribution of Lipid Raft Components

Günter Müller,* Christian Jung, Susanne Wied, Stefan Welte, and Wendelin Frick

Aventis Pharma Germany, 65926 Frankfurt am Main, Germany

Received April 24, 2001; Revised Manuscript Received August 1, 2001

ABSTRACT: The insulin signal transduction cascade provides a number of sites downstream of the insulin receptor (IR) for cross-talk from other signaling pathways. Tyrosine phosphorylation of the IR substrates IRS-1/2 and metabolic insulin-mimetic activity in insulin-responsive cells can be provoked by soluble phosphoinositolglycans (PIG), which trigger redistribution from detergent-insoluble glycolipid-enriched raft domains (DIGs) to other areas of the plasma membrane and thereby activation of nonreceptor tyrosine kinases (NRTK) [Müller, G., Jung, C., Wied, S., Welte, S., Jordan, H., and Frick, W. (2001) *Mol. Cell. Biol.* 21, 4553−4567]. Here we describe that stimulation of glucose transport in isolated rat adipocytes by a different stimulus, the sulfonylurea glimepiride, is also based on IRS-1/2 tyrosine phosphorylation and downstream insulin-mimetic signaling involving activation of the NRTK, $pp59^{Lyn}$, and $pp125^{Fak}$, as well as tyrosine phosphoryation of the DIGs component caveolin. As is the case for PIG 41, glimepiride causes the concentration-dependent dissociation of $pp59^{Lyn}$ from caveolin and release of this NRTK and the glycosyl-phosphatidylinositol-anchored (GPI) proteins, Gce1 and 5′-nucleotidase, from total and anti-caveolin-immunoisolated DIGs. This results in their movement to detergent-insoluble raft domains of higher buoyant density (non-DIGs areas). IRS-1/2 tyrosine phosphorylation and glucose transport activation by both glimepiride and PIG are blocked by introduction into adipocytes of the caveolin scaffolding domain peptide which mimicks the negative effect of caveolin on $pp59^{Lyn}$ activity. Tyrosine phosphorylation of the NRTK, IRS-1/2, and caveolin as well as release of the NRTK and GPI proteins from DIGs and their redistribution into non-DIGs areas in response to PIG is also inhibited by treatment of intact adipocytes with either trypsin *plus* salt or *N*-ethylmaleimide (NEM). In contrast, the putative trypsin/salt/NEM-sensitive cell surface component (CIR) is not required for glimepiride-induced glucose transport, IRS-1/2 tyrosine phosphorylation, and redistribution of GPI proteins and NRTK. The data suggest that CIR is involved in concentrating signaling molecules at DIGs vs detergent-insoluble non-DIGs areas. These inhibitory interactions are relieved in response to putative physiological (PIG) or pharmacological (sulfonylurea) stimuli via different molecular mechanisms (dependent on or independent of CIR, respectively) thereby inducing IR-independent positive cross-talk to metabolic insulin signaling.

A number of physiological, pharmacological, and biochemical stimuli have been reported to increase glucose uptake and metabolism in a variety of primary and cultured mammalian cells. Glucose transport activation by many (e.g., insulin), but not all, stimuli (e.g., exercise) is accompanied by increases in phosphatidylinositol 3-kinase (PI-3K)[1] activity (*1*−*3*). Stimulation of glucose disposal by insulin requires the activation of PI-3K inducing elevated activity of PIP_3-dependent kinases such as protein kinases PDK, PKB, and PKC (isoforms ζ/λ)(*4*, *5*). Most metabolic actions of insulin, including activation of glucose transport and metabolism, are blocked by PI-3K inhibitors, such as wortmannin, or by dominant-negative PI-3K mutants (*2*, *6*). However, despite the general agreement on the necessity of increased PI-3K activity for insulin-stimulated glucose transport, it is now clear that additional signals are required. (i) Cell-permeable PIP_3 analogues fail to elevate glucose transport (*7*). (ii) Two naturally occurring IR mutations which retained the ability of fully activating PI-3K are inactive in mediating glucose transport upregulation (*8*). (iii) PDGF, interleukin-4 and engagement of integrin receptors do not effect glucose transport, although they stimulate PI-3K (*9*, *10*). These stimuli/mutant IR stimulate PI-3K, as does insulin and wild-type IR by inducing tyrosine phosphorylation of IRS (*11*) which bind to and activate PI-3K.

* To whom correspondence should be addressed. Phone: +4969-305-4271. Fax: +4969-305-81901. E-mail: Guenter.Mueller@aventis.com.

[1] Abbreviations: CBD(P), caveolin-binding domain (peptide); CIR, trypsin/salt/NEM-sensitive cell surface component involved in redistribution of DIGs components; CSD(P), caveolin-scaffolding domain (peptide); DIGs, detergent-insoluble glycolipid-enriched raft domains; eNOS, endothelial nitric oxide synthase; Gce1, GPI-anchored cAMP-binding ectoprotein-1; (G)SL (glyco)sphingolipids; GPI, glycosyl-phosphatidylinositol; GPI protein, GPI-anchored plasma membrane protein; IR(β), insulin receptor (β-subunit); IRS(−1/2), insulin receptor substrate proteins (1/2); KRH, Krebs-Ringer-Hepes-based buffer; NEM, *N*-ethylmaleimide; NRTK, non-receptor tyrosine kinase(s); Nuc, 5′-nucleotidase; PI 3-kinase, phosphatidylinositol 3-kinase; PIG, phosphoinositolglycans; PIP_3, phosphatidylinositol-trisphosphat; PKB/C, protein kinase B/C; SDS−PAGE, sodium dodecyl sulfate−polyacrylamide gel electrophoresis; TX-100, Triton X-100.

10.1021/bi0108352 CCC: $20.00
Published on Web 11/07/2001

There are two putative explanations for the apparent lack of coupling of tyrosine-phosphorylated IRS and bound/activated PI-3K to downstream signaling to the glucose transport system. (i) The wild-type IR phosphorylates the IRS at tyrosine residues in addition to those required for PI-3K binding which are not affected by the mutant IR or the PDGF, cytokine and integrin stimuli. In fact, IRS-1 harbors 18 putative tyrosine phosphorylation sites (*1*, *11*) in amino acid sequence motifs that directly bind to SH2 domains in several adaptor/regulatory proteins, including p85 of PI-3K, Grb-2, Nck, Crk, PLCγ, SHP-2. Those phosphorylated in response to factors other than insulin have not been determined so far. (ii) The wild-type IR phosphorylates substrates in addition to IRS, e.g., caveolin or Cbl (*12*−*14*). Recently, a candidate pathway for generation of a second IRS- and PI-3K-independent insulin signal to the glucose transport system has been identified (*14*, *15*). It emerges from DIGs, spezialized domains of the plasma membrane with distinct structure and functions, and is based on the in- and out-movement of signaling proteins.

DIGs can be isolated as low-density, TX-100-insoluble membrane complexes that are enriched in (G)SL, cholesterol, and GPI proteins (*16*). Studies with model systems suggest that DIGs represent liquid-ordered phases with reduced membrane fluidity (*17*). DIGs have been proposed to be involved in membrane trafficking, cell morphogenesis, and signal transduction mechanisms (*18*, *19*). A variety of signaling molecules are concentrated at DIGs, including NRTK of the Src family, heterotrimeric and Ras-like G proteins, cell surface receptors, and Ca^{2+} channels/transporters. The existence of DIGs in situ is strongly supported by the clustered distribution of GPI proteins and GSL, recently visualized under appropriate fixation conditions (*20*) and their confined diffusion in the plasma membrane (*21*). In situ, DIGs may be related in terms of composition and/or topography to caveolae, originally defined as flask- or bulb-shaped invaginations (50−100 nm diameter) of the plasma membrane found in many differentiated cells, such as endothelial, epithelial, muscle, and adipose cells (*18*, *22*−*24*). It has been shown that DIGs can be detected as caveolae-independent structures in cells that either contain or are devoid of caveolae. In cells lacking morphologically recognizable caveolae, such as lymphocytes and certain neuronal and hematopoetic cells, the concentration of (G)SL, cholesterol, GPI proteins, and signaling molecules (e.g., NRTK) in DIGs has been clearly demonstrated (*25*). Caveolins, 21−25-kDa integral membrane proteins (*26*) with isoforms 1 and 2 ubiquitously expressed and isoform 3 expressed in muscle (*19*, *24*), are the structural and marker proteins of caveolae and are dramatically enriched in DIGs. Direct binding of cholesterol to caveolin may stabilize the generation of caveolin homooligomers, which upon interaction with each other within DIGs drive the formation of invaginated caveolae (*27*). Thus, DIGs lacking caveolin may represent the biogenetic precursors for caveolae (precaveolae or caveolae-related microdomains), and DIGs containing caveolin can be considered as the biochemical correlate of caveolae (*23*, *28*).

In 3T3-L1 adipocytes, the protooncogene Cbl is bound to the adaptor protein CAP via association of the carboxy-terminal SH3 domain of CAP with a proline-rich domain in Cbl (*13*, *14*). CAP expression correlates well with insulin sensitivity in insulin-responsive cells and is upregulated during adipocyte differentiation (*29*). The Cbl/CAP complex is targeted to the IR in the basal state but migrates to DIGs upon tyrosine phosphorylation by the IR (*14*, *15*). The interaction of the Cbl-CAP complex with DIGs is mediated by flotillin, another resident and structural protein of DIGs/caveolae (*30*). Overexpression of a dominant-negative CAP mutant (lacking the SH3 domain) in 3T3-L1 adipocytes leads to inhibition of the ternary complex formation and thereby of translocation of Cbl-CAP to DIGs. This leads to complete blockade of insulin-stimulated glucose transport despite functionality of the PI-3K pathway (*15*). The translocation of phosphorylated Cbl recruits additional signaling proteins, such as the GDP/GTP exchange factor C3G, to DIGs resulting in activation of the G protein TC10. This may ultimately provide the second PI-3K-independent signal for glucose transport stimulation by insulin. Thus, DIGs seem to harbor insulin signaling components and to regulate their activity by interaction with flottilin.

Considering the noninsulin glucose transport stimuli which use the PI-3K pathway, one may assume that these manage to elicit the same set of substrate tyrosine phosphorylations (e.g., Cbl) as provoked by insulin in addition those required for PI-3K stimulation (IRS). Previously, we demonstrated that two factors structurally totally different from one another, synthetic PIG and the sulfonylurea glimepiride, potently activate glucose transport and non-oxidative glucose metabolism in primary and cultured adipocytes, diaphragms and cardiomyocytes (*31*−*34*). (i) Hydrophilic PIG induce tyrosine phosphorylation of IRS-1/2 and PI-3K activation (*32*, *35*) by activating the Src family NRTK, $pp59^{Lyn}$ (*36*). In the basal state, this dual-acylated NRTK is associated with caveolin via the interaction of the CSD of caveolin with the CBD of $pp59^{Lyn}$ and is thereby kept in the inactive state (*37*). In response to PIG, $pp59^{Lyn}$ dissociates from caveolin resulting in its activation. Interestingly, introduction of a synthetic peptide corresponding to the CSD blocks $pp59^{Lyn}$ activation and PIG-stimulated but not insulin-stimulated glucose transport (*37*). Thus, the DIGs-caveolin-$pp59^{Lyn}$ pathway, which is required for PIG but not insulin signaling to the glucose transport system, may succeed in inducing all the tyrosine phosphorylation events downstream of IR at the level of both IRS-1/2 and the other substrate proteins typical for insulin. (ii) The blood glucose-lowering lipophilic sulfonylurea drug, glimepiride (*38*, *39*), increases glucose transport and metabolism to a limited degree without causing activation of the IR (*33*, *34*, *40*−*42*) but in close correlation to tyrosine phosphorylation of caveolin and to direct interaction of the drug with glycolipids residing in DIGs (*43*, *44*). The IR-independent glimepiride signaling pathway to the glucose transport system including the putative involvement of IRS tyrosine phosphorylation and PI-3K activation has not been elucidated so far, but may rely on the DIGs-caveolin-$pp59^{Lyn}$ pathway which is used by PIG.

Here we present evidence that, in isolated rat adipocytes, glimepiride actually causes tyrosine phosphorylation of IRS-1/2 and consequent downstream signaling to the glucose transport system via release from DIGs and caveolin of $pp59^{Lyn}$ resulting in its activation. Thus, the DIGs-caveolin-$pp59^{Lyn}$ pathway engaged by both glimepiride and PIG stimulate the PI-3K-dependent (via IRS-1/2) and, in addition, may stimulate the PI-3K-independent pathway (possibly via

Cbl) mediating metabolic insulin-mimetic action. Upregulation of $pp59^{Lyn}$ by its redistribution from DIGs to detergent-insoluble non-DIGs areas apparently substitutes for IR activation. The redistribution process per se rather than the underlying molecular mechanism is critical for the cross-talk to the metabolic insulin signaling cascade, since inactivation of a trypsin/salt/NEM-sensitive plasma membrane component in adipocytes blocks the migration/dissociation of signaling proteins from DIGs/caveolin as well as downstream insulin-mimetic signaling in response to PIG but not glimepiride.

EXPERIMENTAL PROCEDURES

Materials. Anti-CT-PKBα antibody (1:2000 dilution; immunoaffinity-purified, generated in sheep against a peptide corresponding to aa 466−480 of rat PKBα) and anti-phospho-PKBα(Thr308) antibody (1:500 dilution; immunoaffinity-purified, generated in rabbits against a peptide corresponding to aa 301−312 of mouse PKBα and containing phosphothreonine at position 308) were delivered by Upstate Biotechnology (Lake Placid, NY). Anti-caveolin-1 antibody (1:500 dilution; monoclonal, clone C060, raised against a peptide corresponding to aa 1−97 of human caveolin-1) was purchased from Transduction Laboratories (Lexington, KY), anti-Nuc antibody (1:750 dilution, polyclonal, raised against purified soluble rat liver Nuc [cleaved by bacterial PI-specific phospholipase C] were obtained from Dr. M. Remlinger (University Munich, Germany). All other materials were obtained as described (*31*−*37*, *45*).

Preparation of Rat Adipocytes and Incubation with PIG/Sulfonylureas. Adipocytes were isolated by collagenase digestion from epididymal fat pads of male Sprague−Dawley rats (140−160 g, fed ad libitum) and incubated in KRH (0.12 M NaCl, 4.7 mM KCl, 2.5 mM $CaCl_2$, 1.2 mM $MgSO_4$, 1.2 mM KH_2PO_4, 20 mM Hepes/KOH, pH 7.4, containing 2% (w/v) BSA, 100 μg/mL gentamycin, 100 nM 1-methyl-2-phenylethyladenosine, 0.5 units/mL adenosine deaminase, 0.5 mM sodium pyruvate and 5 mM D-glucose) in the presence of PIG (dissolved in 20 mM Hepes/KOH, pH 7.4) or glimepiride (dissolved as a 10 mM stock solution made daily by suspending 9.95 mg of glimepiride in 1.94 mL of aqua bidest., followed by addition of 60 μL of 1 N NaOH and warming up to 50−70 °C) or were electroporated with peptides (dissolved in DMSO at 30 mM, final DMSO concentration 1% which was also contained in control incubations and did not affect adipocyte viability), at 37 °C in a shaking water bath at constant bubbling with 5% CO_2/95% O_2 for the periods indicated (*33*, *36*, *45*).

Preparation of DIGs and non-DIGs Areas. DIGs were routinely isolated from PIG/glimepiride-stimulated adipocytes using the detergent method (*36*, *37*). Separation of detergent-insoluble glycolipid rafts into DIGs and non-DIGs areas was accomplished by the carbonate method and subsequent sucrose gradient centrifugation as described previously (*36*, *37*). Briefly, plasma membranes were suspended in 1.5 mL of 0.5 M Na_2CO_3 (pH 11) and sonicated. The suspension was then adjusted to 45% sucrose in 15 mM Mes/KOH (pH 6.5), 75 mM NaCl, 0.25 M Na_2CO_3, overlayed with 2 mL each of 35, 25, 15, and 5% sucrose in the same medium, and centrifuged (230000*g*, Beckman SW41 rotor, 18 h). Gradient fractions of 0.85 mL were collected to yield a total of 14 fractions. The individual gradient fractions were pooled into DIGs (fractions 4−7) and non-DIGs areas (fractions 10−14). The raft domains from the pooled gradient fractions were diluted 5−10-fold with 25 mM Mes (pH 6.5), 150 mM NaCl, 1% TX-100, collected by centrifugation (50000*g*, 30 min, 4 °C) and resuspended in nondissociating buffer (10 mM Tris/HCl, pH 7.4, 150 mM NaCl, 1% Nonidet P-40, 5 mM EDTA, 0.5 mM EGTA, 1 mM sodium orthovanadate, 50 mM NaF, and protease inhibitors) or dissociating buffer (= nondissociating buffer supplemented with 60 mM β-octylthioglucoside, 0.3% deoxycholate) as indicated, incubated (1 h, on ice) and used for (co)immunoprecipitation, immunoblotting, or photoaffinity labeling.

Treatment with Trypsin plus Salt or NEM of Rat Adipocytes. For trypsin/salt treatment, 2.5 mL of adipocyte suspension (3.5×10^6 cells/mL) in KRH containing 5 mM glucose was incubated (20 min, 30 °C) in the presence of 100 μg/mL trypsin. After addition of soy bean trypsin inhibitor (final concentration 100 μg/mL) and 2.5 mL of KRH containing 1 M NaCl and 0.5% BSA and further incubation (10 min, 22 °C), the cells were centrifuged (1500*g*, 5 min, swing-out rotor). For NEM treatment, 1 mL of adipocyte suspension (3.5×10^6 cells/mL) in KRH containing 5 mM glucose was incubated (30 min, 22 °C) with NEM (1.5 mM final concentration) and then with DTT (15 mM final concentration, 5 min, 15 °C). After removal of the infranatant, the cell suspension of both treatments (about 0.5 mL) was supplemented with 10 mL of KRH containing 0.5% BSA and then centrifuged again (500*g*, 1 min, swing-out rotor). After two additional washing steps, the final cell suspension was adjusted to 25 mL of KRH containing 0.5% BSA, 50 μM glucose, and 1 mM sodium pyruvate. Portions or 0.2 mL were assayed for lipogenesis to monitor the loss of responsiveness toward PIG 41 (see ref *46*). Control cells received water instead of trypsin/NaCl/NEM and were subjected to the same centrifugation and washing procedures as the treated cells.

Preparation of the Trypsin/Salt-Extract. For preparation of the extract from intact adipocytes, 10 mL of adipocyte suspension (3.5×10^6 cells/mL) in KRH containing 5 mM glucose and 0.5% BSA was incubated (20 min, 22 °C) with 100 μg/mL trypsin. After addition of 10 mL of KRH containing 1 M NaCl, 100 μg/mL soy bean trypsin inhibitor, 1 mM PMSF, 25 mM benzamidine, 2 μM leupeptin, 5 μM pepstatin and 10 μg/mL antipain, the cells were centrifuged (1500*g*, 5 min, swing-out rotor). The infranatant was removed by aspiration, dialyzed (4 × 500 mL of 25 mM Hepes/KOH, pH 7.4, 1 mM EDTA, 5% glycerol, 0.2 mM PMSF, overnight), and then supplemented with the same volume of ice-cold 25% poly(ethylene glycol) 6000 in the same buffer. After incubation (2 h, 4 °C), the precipitates were collected by centrifugation (48000*g*, 30 min, 4 °C), washed twice with 6% poly(ethylene glycol) 6000, and stored in liquid nitrogen until use.

Reconstitution of Trypsin/Salt-Treated Adipocytes. The precipitated trypsin/salt extract was dissolved in 1 mL of 25 mM Hepes/KOH (pH 7.4), 1 mM EDTA, 1 M NaCl. One milliliter of extract was added to 1-mL portions of adipocyte suspension (3.5×10^6 cells/mL of KRH containing 5 mM glucose, 1% BSA). The reconstitution was initiated by supplementation with 8 mL of KRH containing 5 mM glucose. After incubation (1 h, 22 °C) under an atmosphere

of 95% O_2/5% CO_2, the cells were centrifuged (500*g*, 1 min, swing-out-rotor), washed twice with KRH and finally suspended in 10 mL of KRH containing 1% BSA, 50 μM glucose and 1 mM sodium pyruvate for assaying PIG-dependent lipogenesis (0.2-mL aliquots) to monitor successful reconstitution (see ref *46*).

Photoaffinity Labeling. Solubilized plasma membranes and DIGs (5−10 μg of protein) were incubated (30 min, 4 °C) with 50 μCi of 8-N_3-[^{32}P]cAMP (0.5 nmol) in 50 μL of 10 mM Tris/HCl (pH 7.4), 1 mM EDTA, 0.5 mM EGTA, 140 mM NaCl, 10 mM $MgCl_2$, 2 mM $MnCl_2$, 1 mM isobutylmethylxanthine, 1 mM DTT, 1 mM AMP, and protease inhibitors in the wells of microtiter plates (96-formate) and then irradiated with UV light (254 nm, 8000 μW/cm^2) at a distance of 0.5 cm for 1 min (*47*, *48*). Subsequently, the photoaffinity labeling reaction was quenched by addition of 100 μL of the same buffer containing 10 mM cAMP. Gce1 was precipitated (5% trichloroacetic acid, 1 h on ice, 10000*g* for 15 min) and solubilized in sample buffer for SDS−PAGE. Radiolabeled Gce1 was visualized by phosphorimaging.

Glucose Transport. Glucose transport was assayed as described (*33*, *45*). Washed adipocytes (two cycles with KRH containing 0.5% BSA) were incubated with 2-deoxy-D-[2,6-^{3}H]glucose (50 μM, 0.33 μCi/mL; 20 min at 37 °C) in the absence or presence of 10 μM cytochalasin B and then centrifuged through a oil layer prior to liquid scintillation counting.

Immunoprecipitation. Total cell lysates (25−50 μg of protein) or DIGs in nondissociating/ dissociating buffer (10−15 μg protein) were precleared (1 h, 4 °C) with protein G/A-Sepharose (50 mg/mL) in a total volume of 100 μL and then supplemented with appropriate antibodies (pp125^{Fak}, 2 μg/sample; IRS-1, 1:50 dilution; IRS-2, 10 μg/sample; pp59^{Lyn}, 5 μg/sample; caveolin-1, 0.7 μg/sample; IRβ, 1:175 dilution) preadsorbed on protein G-Sepharose (monoclonal antibodies) or protein A-Sepharose (rabbit antibodies) in a total volume of 100 μL. After incubation (4 h, 4 °C, end-over-end rotation) and centrifugation (3000*g*, 2 min, 4 °C), the collected immune complexes were washed twice with 1 mL each of immunoprecipitation buffer (50 mM Hepes/KOH, pH 7.4, 500 mM NaCl, 100 mM NaF, 10 mM EDTA, 10 mM sodium pyrophosphate, and 1 mM sodium orthovanadate) containing 0.2% Nonidet P-40 and 0.3% deoxycholate, then twice with 1 mL each of immunoprecipitation buffer containing 150 mM NaCl and 0.2% Nonidet P-40 and once with 1 mL of immunoprecipitation buffer lacking salt and detergent and finally suspended in 50 μL of Laemmli buffer (4% SDS, 115 mM Tris/HCl, pH 6.8, 1 mM EDTA, 10% glycerol, 4 mg/mL bromo-phenol blue) supplemented with 1.2% β-mercaptoethanol (except for anti-caveolin immunoprecipitates), heated (95 °C, 2 min), and centrifuged. The supernatant samples were analyzed by SDS−PAGE (4−12% Bis-Tris precast gel, pH 6.4, Mes/SDS running buffer) under reducing conditions. The centrifugation conditions used for collection of the protein A/G Sepharose-bound immune complexes did not lead to sedimentation of nondissociated DIGs to any significant degree according to caveolin immunoblotting. The coimmunoprecipitation of proteins with caveolin from dissociated DIGs was specific for caveolin-interacting DIGs components, such as pp125^{Fak} and pp59^{Lyn}. They were not immunoprecipitated using nonimmune IgG instead of anti-caveolin antibody. In contrast, Gce1 was recovered only from nondissociated DIGs either directly or via coimmunoprecipitation with caveolin. Caveolin immunoprecipitates from dissociated DIGs did not contain appreciable amounts of Gce1. This is compatible with localization of Gce1 in DIGs on basis of interactions between its GPI anchor/protein moiety and lipid/polypeptide constituents (e.g., receptor) at DIGs rather than directly between its GPI anchor and caveolin (see ref *37*).

Immunoblotting. Immunoblotting was performed as described previously (*35*, *36*) with minor modifications. Briefly, after SDS−PAGE and transfer of the proteins to polyvinylidene difluoride membranes (2 h, 400 mA in 20% methanol, 192 mM glycine, 25 mM Tris, 0.005% SDS), the blocked membrane [1 h in 20 mM Tris/HCl, pH 7.6, 150 mM NaCl, 0.05% Tween 20, 0.1% Brij, 0.01% Nonidet P-40 supplemented with 1% ovalbumin and 1% BSA (anti-phosphotyrosine, anti-pp59^{Lyn}, anti-IRβ) or with 5% nonfat dried milk (anti-caveolin, anti-pp125^{Fak}, anti-IRS-1/2)] was incubated (2 h, 25 °C) with antibodies against pp125^{Fak} (1:200), IRS-1 (1:500), IRS-2 (1:750), caveolin-1 (1:2000), pp59^{Lyn} (1 μg/mL), or IRβ (2 μg/mL) diluted in the same medium and then washed five times with the same medium. After incubation of the membranes (1 h, 25 °C) with horseradish peroxidase-coupled goat anti-mouse IgG antibody or goat anti-rabbit IgG antibody diluted in the appropriate blocking buffer (1:5000 or 1:2500) and subsequent washing with detergent-containing (see above, two times) and detergent-free (two times) buffer (20 mM Tris/HCl, pH 7.6, 150 mM NaCl), the labeled proteins were visualized by the enhanced chemiluminescence method.

Miscellaneous. Synthesis of the peptides CBDP and CSDP (*37*), electroporation of isolated rat adipocytes with CBDP and CSDP (*36*, *37*), preparation of total adipocyte lysates and plasma membranes (*33*, *36*, *37*, *47*, *48*), immune complex kinase assays (*37*), analysis of caveolin tyrosine phosphorylation (*44*) and SDS−PAGE (*36*) have been performed as described previously. Protein concentration was determined using the BCA protein determination kit from Pierce (Rockford, IL) with BSA used for calibration. Chemiluminescent detection using ECL reagents (Amersham, Freiburg, Germany) and the LumiImager system (Roche Molecular Diagnostics, Penzberg, FRG) was performed according to the manufacturers' instructions. Autoradiographs and phosphorimages were processed and quantified by computer-assisted video densitometry using the Storm 860 PhosphorImager system (Molecular Dynamics, Gelsenkirchen, FRG). Figures of phosphor- and chemiluminescent images were constructed using the Adobe Photoshop software (Adobe Systems Inc., Mountain View, CA).

RESULTS

Recent studies have demonstrated that insulin-mimetic action by PIG in isolated rat adipocytes depends on the presence of CIR at the cell surface which is inactivated by combined trypsin/salt or NEM action (*46*). Incubation of intact isolated rat adipocytes with 100 μg/mL (final concentration) trypsin and subsequent washing of the cells with 0.5 M NaCl or treatment of the adipocytes with 1.5 mM NEM resulted in 30−70% reduction of glucose transport activation at 1−10 μM PIG 41 as assayed after removal of trypsin,

Table 1: Differential Effect of Inactivation of CIR on PIG- and Glimepiride-Induced Glucose Transport[a]

	[μM]	0.1 μM	0.3 μM	1 μM	3 μM	10 μM
control	PIG 41	6.7 ± 0.5	12.4 ± 1.8	44.8 ± 6.1	84.6 ± 6.5	100 ± 7.7
	Gli	8.6 ± 0.7	8.1 ± 1.0	34.7 ± 4.6	69.4 ± 4.8	100 ± 6.2
NaCl	PIG 41	6.6 ± 1.7	14.7 ± 1.5	52.3 ± 4.9	89.3 ± 7.1	110.4 ± 9.7
trypsin	PIG 41	8.3 ± 1.4	16.8 ± 1.3	56.7 ± 3.8	91.4 ± 6.9	114.4 ± 8.8
trypsin + NaCl	PIG 41	24.9 ± 1.7	28.0 ± 1.5	32.5 ± 1.8	45.3 ± 3.3	44.5 ± 2.9
	Gli	24.0 ± 0.5	29.1 ± 1.3	36.9 ± 5.2	74.4 ± 5.9	96.7 ± 8.3
NEM	PIG 41	21.4 ± 0.8	25.1 ± 1.8	38.9 ± 3.1	46.4 ± 4.8	49.6 ± 3.7
	Gli	24.5 ± 0.9	30.2 ± 1.5	41.6 ± 3.9	70.8 ± 5.1	107.6 ± 9.4
NEM + DTT	PIG 41	8.9 ± 1.1	14.7 ± 1.0	40.2 ± 3.1	78.4 ± 5.9	95.3 ± 7.7

[a] Isolated rat adipocytes were incubated in the absence (Control) or presence of NaCl, trypsin, trypsin *plus* NaCl, NEM or NEM *plus* DTT (see Experimental Procedures). Subsequently, the adipocytes were incubated (20 min, 37 °C) in the absence or presence of increasing concentrations of PIG 41 or glimepiride (Gli) as indicated and then assayed for 2-deoxyglucose transport. Quantitative evaluations of three different adipocyte incubations with measurements in quadruplicate each (mean ± SD) are given as a percentage of maximal glucose transport (difference between 10 μM PIG 41/glimepiride and basal) which is set at 100% in each case and was 3.7-fold higher for PIG 41 compared to glimepiride.

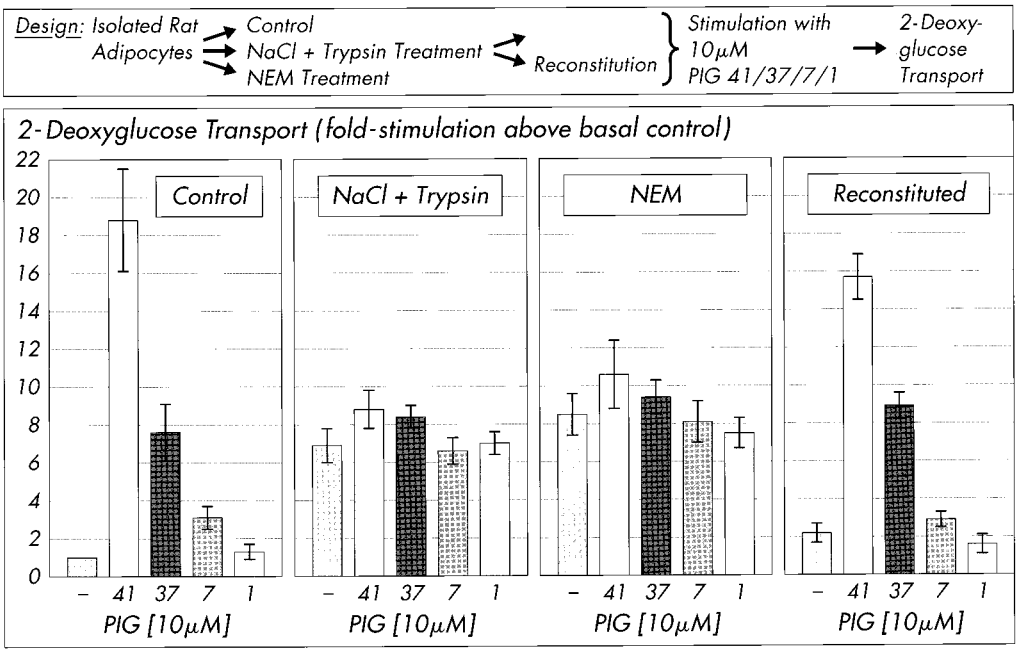

FIGURE 1: Inactivation of CIR induces constitutive glucose transport. Isolated rat adipocytes were incubated in the absence (Control) or presence of trypsin *plus* NaCl or NEM (see Experimental Procedures). A portion of the trypsin/NaCl-treated adipocytes was subjected to reconstitution with trypsin/NaCl-extract. The four portions of adipocytes were incubated (20 min, 37 °C) in the absence or presence of 10 μM PIG 41, 37, 7, and 1 and then assayed for 2-deoxyglucose transport. Quantitative evaluations of four different adipocyte incubations with measurements in quadruplicate each are given as fold stimulation (mean ± SD) with basal values (absence of PIG) for the control cells set at 1.

salt, and NEM (Table 1, Figure 1). Basal glucose transport was increased 7−8-fold in trypsin/salt- or NEM-treated adipocytes compared to control cells approaching and even exceeding the maximal stimulation by the structurally related but less potent PIG derivatives (*32*), PIG 7 and 37 (at 10 μM) (Figure 1). The derivative PIG 1 was used as a negative control to demonstrate specificity. Treatment of intact adipocytes with trypsin alone or NaCl alone or NEM in the presence of DTT did not significantly affect both basal and PIG-stimulated glucose transport demonstrating that the incubation/washing conditions per se do not lead to stress activation of the glucose transport system or blockade of PIG signaling. Remarkably, addition of trypsin/salt-extract containing CIR to trypsin/salt-treated adipocytes and subsequent lowering of the NaCl concentration restored PIG-stimulated glucose transport in the reconstituted cells (Figure 1, Table 1). This strongly argues for the specificity of inactivation of CIR and its requirement for insulin-mimetic metabolic PIG action. In contrast, the concentration-dependent activation of glucose transport by glimepiride was not affected by trypsin/salt or NEM treatment of the adipocytes (Table 1).

The insulin-mimetic activity of glimepiride in insulin-responsive cells in vitro is reflected in (i) stimulation of glucose transport in normal and insulin-resistant isolated rat adipocytes (to up to 40% of the maximal insulin response at 10 μM; see ref *33*), cultured 3T3-L1 adipocytes (*34*), and isolated rat cardiomyocytes (*40*) based on elevated translocation of glucose transporter molecules from intracellular vesicles to the plasma membrane (*33*), (ii) upregulated expression of glucose transporter molecules (*40*), (iii) increase of non-oxidative glucose metabolism in response to modulation of the activity of key regulatory enzymes, and (iv) inhibition of lipolysis based on lowering of cytosolic cAMP (*34*). So far, there is no evidence that glimepiride activates the IR tyrosine kinase (*43*) raising the question on the molecular mechanism(s) of its pleiotropic effects and

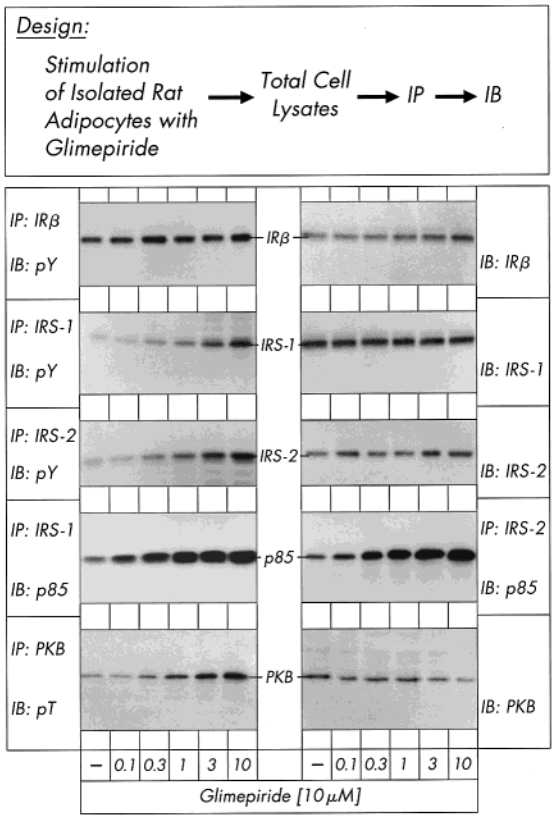

FIGURE 2: Glimepiride induces insulin-mimetic signaling without activating IR. Isolated rat adipocytes were incubated (20 min, 37 °C) with increasing concentrations of glimepiride. IRβ, IRS-1/2, and PKB were immunoprecipitated from total cell lysates and then probed for phosphotyrosine (pY), p85 subunit of PI-3K (p85), or phosphothreonine 308 of PKB (pT) by immunoblotting using chemiluminescent detection. The efficiency of each immunoprecipitation was analyzed by homologous immunoblotting. The figure shows representative blots/chemiluminescent images repeated two to four times with similar results.

signal convergence upstream of the glucose transport and diverse metabolic effector systems. Interestingly, incubation of isolated rat adipocytes with glimepiride (0.1−10 μM) induced pronounced tyrosine phosphorylation of IRS-1 and IRS-2, association of the regulatory p85 subunit of PI-3K with IRS-1 and IRS-2 as well as phosphorylation of PKB at threonine 308 in concentration-dependent fashion (Figure 2). As expected, tyrosine phosphorylation of IRβ was not affected by glimepiride. Comparable recoveries of the individual immunoprecipitations were confirmed by homologous immunoblotting. Thus, the insulin-mimetic metabolic activity of glimepiride seems to be based on the typical insulin-mimetic signaling downstream of tyrosine phosphorylation of IRS-1/2 (by a kinase different from IR) and its binding to and activation of PI-3K. This in turn leads to phosphorylation (at threonine 308) and activation of PKB where the signal apparently diverges to the various metabolic effector systems (*1*, *3*, *11*). Studies with knockout mice suggest that IRS-1 (*49*, *50*) and IRS-2 (*51*) are not functionally interchangeable in tissues that are responsible for glucose production and glucose disposal such as liver and skeletal muscle. Thus, IRS-2 appears to play a major role in regulating hepatic insulin action, whereas in skeletal muscle and adipose tissue, IRS-2 may be unable to entirely compensate for defects in IRS-1 signaling (*52*). Data obtained with mice with combined heterozygous null mutations in IR, IRS-1, and IRS-2 further argue for IRS-1 playing a major role in skeletal muscle and adipose tissue and IRS-2 in liver (*53*). Thus, the engagement of both IRS-1 and IRS-2 during glimepiride signaling (see Figure 2) may explain the pleiotropic insulin-mimetic metabolic activity of this hypoglycemic drug as demonstrated in adipose/muscle/liver tissues in animal studies.

The insulin signaling pathway downstream of IR is also activated by PIG (*35*) which have been reported to exert potent insulin-mimetic metabolic activity in insulin target cells (see Figure 1 and ref *54*). In agreement, in isolated rat adipocytes PIG 41 increased tyrosine phosphorylation of IRS-1/2 (at 0.1 μM to about the same degree as 10 μM glimepiride; Figure 3). Combination of glimepiride and PIG 41 at concentrations which elicit maximal responses each (10 and 1 μM, respectively) did not significantly exceed the tyrosine phosphorylation of IRS-1/2 observed with either stimulus alone, whereas submaximal concentrations (1 and 0.1 μM, respectively) led to about additive effects (Figure 3). This suggests that the signals elicited by glimepiride and PIG converge at IRS-1/2.

Next we studied whether PIG and glimepiride use the same pathway for IRS-1/2 tyrosine phosphorylation a component of which may be CIR. Inactivation of CIR by both trypsin/salt and NEM moderately increased basal but drastically dampened PIG-induced tyrosine phosphorylation of IRS-1/2 (Figure 4, panels A and B). In reconstituted adipocytes, the very low basal tyrosine phosphorylation as well as its pronounced responsiveness toward PIG 41 (to 65−80% compared to mock-treated control cells for IRS-2; to 40−60% for IRS-1) was restored. Thus, inactivation (and reconstitution) of CIR is closely correlated to increased basal/reduced (and restored) PIG-induced tryosine phosphorylation of IRS-1/2 and glucose transport (see Figure 1 and Table 1). As expected, PIG 41 did not elicit tyrosine phosphorylation of IRβ in normal, trypsin/salt-treated, and reconstituted adipocytes to any significant extent (Figure 4, panels A and B). This confirms lack of involvement of CIR in insulin signaling via IRβ and vice versa of IRβ in insulin-mimetic signaling by PIG. Apparently, rather low tyrosine phosphorylation of IRS-1/2 is sufficient (Figure 4, trypsin/salt- or NEM-treated adipocytes in the basal state) to provoke significant glucose transport in isolated rat adipocytes (see Table 1). This is compatible with studies on the correlation of IRS tyrosine phosphorylation and glucose transport in various insulin-responsive cells (*2*, *6*).

Tyrosine phosphorylation of IRS-1/2 in response to glimepiride in isolated rat adipocytes was not impaired by trypsin/salt or NEM treatment or a combination of both (Figure 5). Again, these treatments increased basal IRS-1/2 tyrosine phosphorylation by 30−40% compared to control cells. Insulin-mimetic PIG signaling in adipocytes has been demonstrated to critically depend on the dissociation of the NRTK pp59^{Lyn} from caveolin resulting in its activation (*36*). In fact, pp59^{Lyn} represents a candidate kinase for PIG-dependent IRS-1/2 tyrosine phosphorylation, since it is activated by PIG in intact rat adipocytes and accepts IRS-1/2 as substrate (*36*, *37*). Synthetic CSDP, which corresponds to the region of interaction of caveolin with a number of signaling proteins (for its structure, see ref *37*), introduced into isolated rat adipocytes by electroporation interfered with PIG-stimulated (*37*) and glimepiride-stimulated IRS-1/2

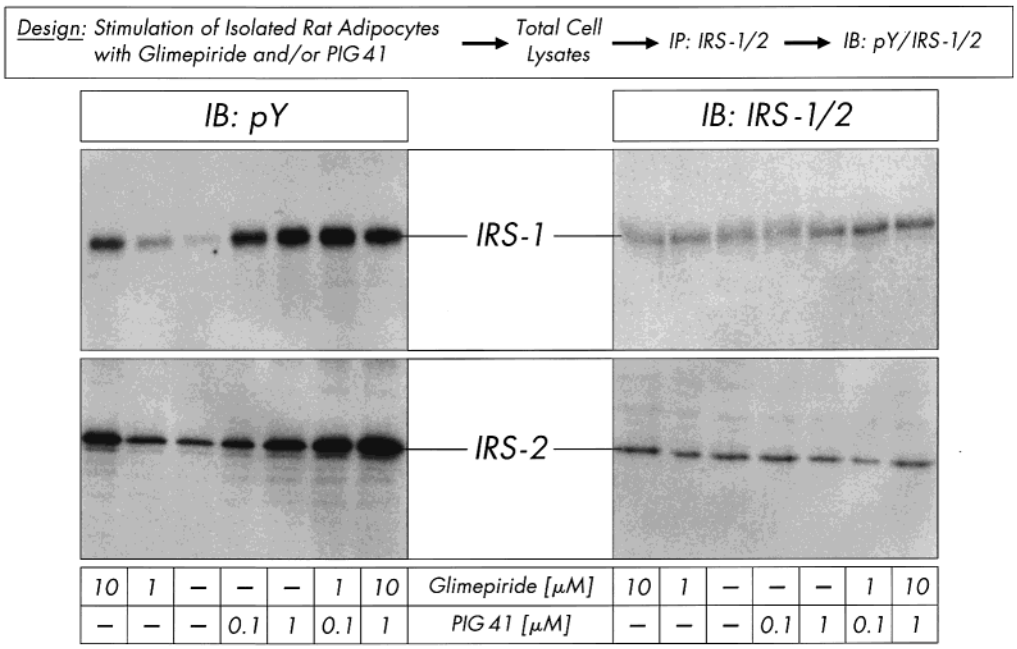

FIGURE 3: Glimepiride and PIG induce IRS tyrosine phosphorylation in additive fashion. Isolated rat adipocytes were incubated (20 min, 37 °C) with different concentrations of glimepiride or PIG 41 or combinations thereof. IRS-1/2 was immunoprecipitated and probed for phosphotyrosine (pY) by immunoblotting using chemiluminescent detection. The efficiency of each immunoprecipitation was analyzed by homologous immunoblotting. Typical blots/chemiluminescent images are shown repeated three times with similar results.

tyrosine phosphorylation (Figure 5) and glucose transport (Table 2) by 55−65 and 45−60%, respectively. This is likely caused by binding of CSDP to the CBD of pp59^{Lyn} thereby mimicking the negative regulatory potential of endogenous caveolin as demonstrated for a variety of protein kinases (*55*−*58*). The blockade of both IRS tyrosine phosphorylation (Figure 5) and glucose transport (Table 2) was abrogated by excess of synthetic CBDP, which corresponds to the putative region of binding of pp59^{Lyn} to CSD (for its structure, see ref *37*), thus competing for the inhibitory pp59^{Lyn}-CSDP interaction. CBDP alone had no effect (Figure 5). Taken together, induction of insulin-mimetic signaling and metabolic action by glimepiride does not depend on CIR, but appears to require the dissociation of signaling proteins, among them NRTK such as pp59^{Lyn} from caveolin. This may lead to their activation. In fact, pp59^{Lyn} and pp125^{Fak} activities recovered from total plasma membranes increased significantly and in concentration-dependent fashion upon incubation of isolated rat adipocytes with glimepiride (Table 3). Stimulation of these NRTK was accompanied by pronounced tyrosine phosphorylation of caveolin-1 with similar dependence on the glimepiride concentration (Table 3). Caveolin-1 may act as substrate for pp59^{Lyn} and pp125^{Fak} in addition to IRS-1/2.

The apparent involvement of pp59^{Lyn} and pp125^{Fak} in insulin-mimetic signaling by PIG and glimepiride prompted us to investigate the role of CIR in regulating NRTK activity. Inactivation of CIR by both trypsin/salt and NEM increased to a limited extent basal but considerably reduced PIG-induced tyrosine phosphorylation of pp59^{Lyn}, pp125^{Fak}, and caveolin (Figure 6, panels A and B). In reconstituted adipocytes, basal tyrosine phosphorylation was reduced to control level and PIG 41-induced tyrosine phosphorylation was restored to 60−85% compared to control cells for pp59^{Lyn} and caveolin and to 45−55% for pp125^{Fak}. Thus, CIR appears to be required for low basal and high PIG-responsive tryosine phosphorylation of pp59^{Lyn}, pp125^{Fak}, caveolin (Figure 6) and IRS-1/2 (Figure 5).

The reported dissociation of pp59^{Lyn} and pp125^{Fak} from caveolin in response to PIG challenge of isolated rat adipocytes (ref *37*) in combination with the observed inhibition of insulin-mimetic signaling by PIG and glimepiride after introduction of CSDP (Figure 5) raised the possibility of a role of CIR in (PIG-dependent) regulation of the localization of signaling components at DIGs. We therefore investigated the impact of inactivation of CIR on the association of DIGs components with caveolin residing in DIGs (Figure 7, panels A and B). DIGs are characterized by a unique lipid composition consisting of cholesterol, (G)SL, and GPI lipids which determines their relative detergent resistance (in the presence of 1% TX-100 at 4 °C for 1 h) and low buoyant density (according to sucrose gradient centrifugation). Their biochemical isolation and purification from mammalian cells and tissues, including adipocytes, have been described previously (*16*, *17*, *20*, *21*, *37*). Treatment of intact rat adipocytes with either trypsin/salt or NEM led to drastic reductions in the amounts of GPI protein Gce1 (by 70−80%, Figure 7A and B), which was coimmunoprecipitated with caveolin from nondissociated DIGs in the basal state. In reconstituted adipocytes, the amount of Gce1 in caveolin immunoprecipitates from nondissociated DIGs approached control levels. Challenge of trypsin/salt- or NEM-treated adipocytes with PIG 41 further decreased the amount of Gce1 from anti-caveolin-immunoisolated nondissociated DIGs by 70−95% (at 10 μM) (Figure 7). In reconstituted adipocytes, PIG 41 provoked loss of Gce1 from anti-caveolin-immunoisolated DIGs to about the same degree and with similar potency (EC_{50} 0.1−0.3 μM) as in control cells. The efficiencies of the individual caveolin immunoprecipitations from nondissociated DIGs as well as Gce1 photoaffinity labelings from total plasma membranes of the differentially pretreated adipocytes in the absence and presence of PIG 41 were

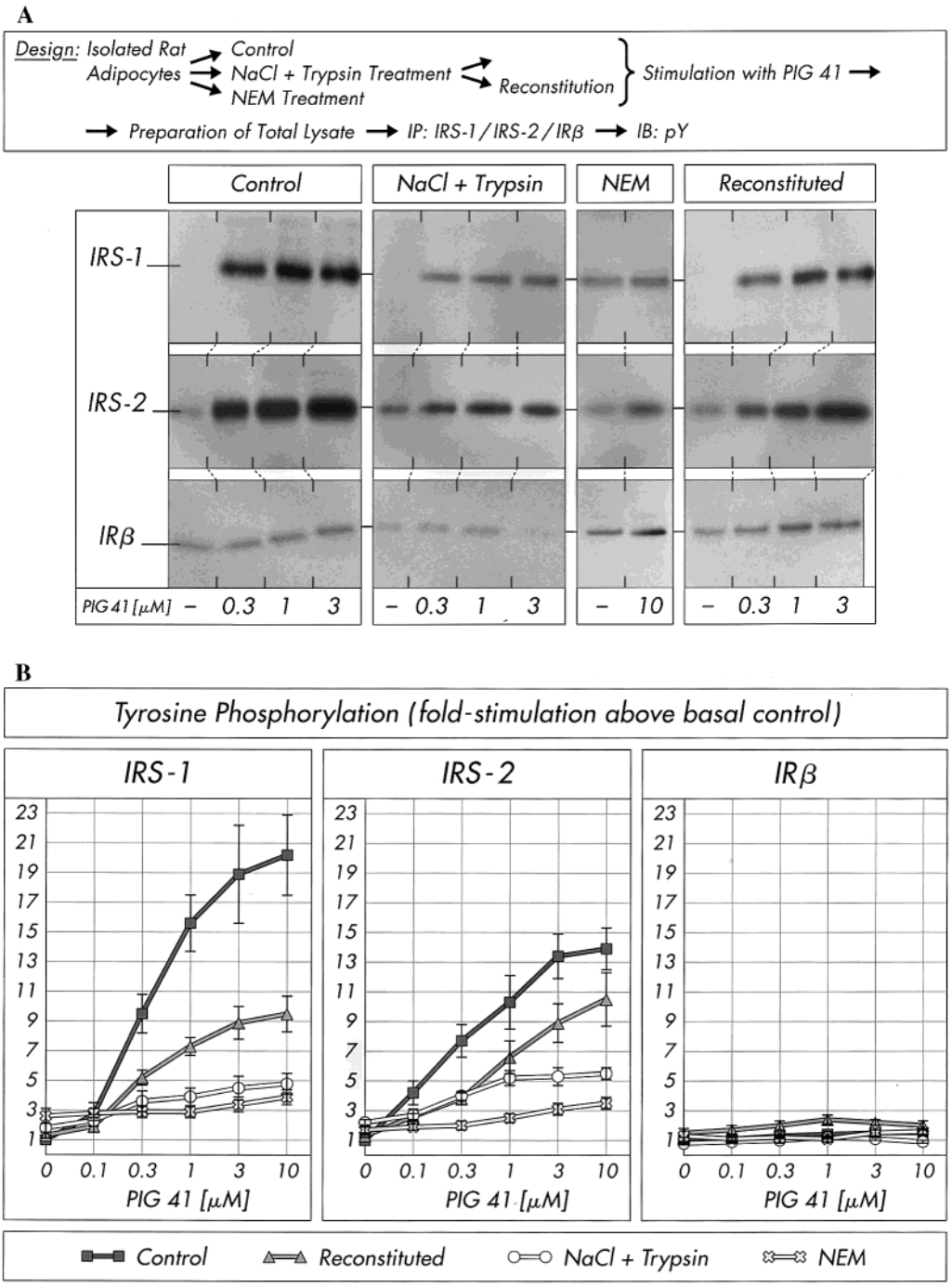

FIGURE 4: Inactivation of CIR inhibits PIG-dependent tyrosine phosphorylation of IRS-1/2. Isolated rat adipocytes were incubated in the absence (Control) or presence of trypsin *plus* NaCl or NEM. Portion of the trypsin/NaCl-treated adipocytes was subjected to reconstitution with trypsin/NaCl-extract. The four portions of adipocytes were incubated (20 min, 37 °C) in the absence or presence of increasing concentrations of PIG 41. Total cell lysates were prepared for immunoprecipitation (IP) of IRS-1/2 and IRβ. The immunoprecipitates were immunoblotted (IB) for phosphotyrosine (pY) using chemiluminescent detection. (A) Chemiluminescent images of a typical experiment are shown repeated two times with similar results. (B) Quantitative evaluations of three different adipocyte incubations with measurements in quadruplicate each are given as fold stimulation (mean ± SD) with basal values (absence of PIG 41) for the control cells set at 1 in each case.

comparable (Figure 7, panels A and B). These data provided first evidence that CIR is involved in the colocalization of GPI proteins, such as Gce1, together with caveolin in DIGs of the adipocyte plasma membrane. Its inactivation (by either trypsin/salt or NEM) and reconstitution (with active CIR) lead to redistribution of a GPI protein from DIGs and to DIGs, respectively. Furthermore, the apparent additive effects of trypsin/salt, NEM and PIG treatment on the redistribution of these components suggest that PIG may regulate their localization at DIGs by reversible inactivation of CIR through an unknown mechanism.

We next studied whether insulin-mimetic signaling by glimepiride is correlated to redistribution of DIGs components. Incubation of isolated rat adipocytes with 10 μM glimepiride considerably reduced the amounts of Gce1, pp125^{Fak}, and pp59^{Lyn} recovered from both total DIGs and caveolin immunoprecipitates from nondissociated DIGs by 60/70, 40/35, and 30/40%, respectively, compared to basal

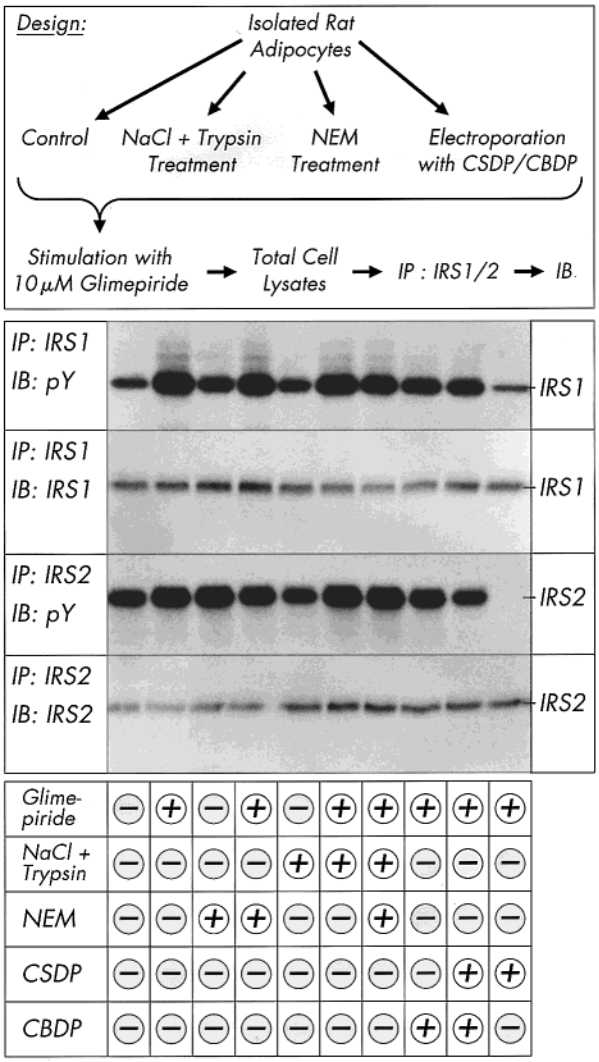

FIGURE 5: CIR is not required for glimepiride-induced insulin-mimetic signaling. Isolated rat adipocytes were incubated in the absence (Control) or presence of trypsin *plus* NaCl or NEM or electroporated with 100 μM CSDP, 300 μM CBDP, or a combination of both (see Experimental Procedures). The four portions of adipocytes were incubated (20 min, 37 °C) in the absence or presence of 10 μM glimepiride as indicated. IRS-1/2 was immunoprecipitated from total cell lysates and probed for phosphotyrosine (pY) by immunoblotting using chemiluminescent detection. The efficiency of the IRS immunoprecipitation was analyzed by homologous immunoblotting. Chemiluminescent images of a typical experiment are shown repeated two times with similar results.

cells (Figure 8, panels A and B). The first generation sulfonylurea, tolbutamide (which does not significantly trigger IRS-1 tyrosine phosphorylation and insulin-mimetic activity; see below and ref *59*) was ineffective even at 100-fold higher concentration than glimepiride (which corresponds to the described therapeutic potency ratio between the two sulfonylureas; see ref *44*). The amounts of IRβ, glucose transporter Glut4 and caveolin (used for normalization of the slightly different efficiencies in the DIGs preparations and immunoprecipitations) in total or anti-caveolin-immunoisolated DIGs was not affected by sulfonylurea treatment. These data argue for the specificity of the glimepiride effect. The apparent redistribution from (caveolin-immunopurified) DIGs of Gce1, pp125^{Fak}, and pp59^{Lyn} in response to glimepiride but not tolbutamide was accompanied by corresponding increments in tyrosine phosphorylation of caveolin and IRS-1/2 in glimepiride- but not tolbutamide-treated adipocytes compared to basal cells (Figure 8, panels A and B). This is correlated to activation of pp125^{Fak} and pp59^{Lyn} and tyrosine phosphorylation of caveolin by glimepiride (Table 3) but not tolbutamide (data not shown).

The concentration-dependent loss of NRTK from caveolin immunoprecipitates obtained from dissociated anti-caveolin-immunoisolated DIGs (pp59^{Lyn}) or nondissociated anti-caveolin-immunoisolated DIGs (pp125^{Fak}) and of Gce1 from total DIGs in response to glimepiride was not significantly impaired upon treatment of isolated rat adipocytes with either trypsin/salt or NEM (Figure 9). Glimepiride and inactivation of CIR did not affect the recovery of caveolin from DIGs, arguing for maintenance of their structural integrity as caveolae. Taken together, these findings suggest that in adipocytes tyrosine phosphorylation of IRS-1/2 in response to glimepiride is mediated via redistribution/activation of pp125^{Fak} and pp59^{Lyn} which occurs independent of CIR. Furthermore, the efficient coimmunoprecipitation of pp59^{Lyn} with anti-caveolin-1 antibodies from dissociated DIGs demonstrates direct interaction of this NRTK with caveolin, presumably mediated by binding of its CBD to CSD rather than a mere colocalization of pp59^{Lyn} and caveolin in DIGs. In contrast, Gce1 and Nuc (data not shown) are efficiently recovered with caveolin immunoprecipitates from nondissociated DIGs but not dissociated DIGs (see Experimental Procedures) arguing for residence of GPI proteins in DIGs which does not rely on direct binding to caveolin. This mode of targeting is compatible with the missing topological relationship between GPI proteins and caveolin, the fatty acyl chains of the GPI protein anchor embedded in the outer leaflet of the DIGs membrane and the hydrophobic membrane-anchoring domain of caveolin traversing the inner leaflet only (*18*, *23*).

Glimepiride was most efficient in triggering redistribution of pp59^{Lyn} from total DIGs in isolated rat adipocytes (92% at 3 μM) followed by the second generation sulfonylureas, glibenclamide (81% at 7.5 μM), gliclazide (46% at 120 μM), and glipizide (22% at 300 μM), whereas tolbutamide (at 1 mM) was virtually inactive (Figure 10). The ratio of the sulfonylurea concentrations used corresponded to that of equipotent blood glucose-lowering doses during treatment of rabbits and rats (*44*). The ranking of the sulfonylureas in inducing movement of pp59^{Lyn} out from DIGs was identical to that of redistribution of Gce1 (Figure 10) and to their relative blood glucose-lowering potency in diverse animal models of type II diabetes and type II diabetic patients (*59*). This may be taken as evidence for operation of the sulfonylurea-induced redistribution process also in vivo and its involvement in promoting insulin-independent peripheral glucose disposal as demonstrated for glimepiride in acute animal studies (*44*, *59*).

The observed release of Gce1 and pp125^{Fak} from anti-caveolin-immunoisolated DIGs and dissociation of pp59^{Lyn} from caveolin immunoprecipitates of PIG- and glimepiride-treated adipocytes raised the question about the subsequent localization of the former free (Gce1, pp125^{Fak}) or caveolin-bound (pp59^{Lyn}) DIGs components. Apparently they are released from DIGs in response to sulfonylureas of the second and third generation as revealed by direct immunoblotting of total DIGs proteins omitting prior caveolin

Table 2: Inhibition of PIG and Glimepiride Stimulation of Glucose Transport by Electroporation of Adipocytes with CSDP[a]

	[μM]	−	0.3 μM	1 μM	3 μM	10 μM
control	PIG	1	1.7 ± 0.2	4.2 ± 0.3	6.9 ± 0.4	7.8 ± 0.5
	Gli	1	0.9 ± 0.1	1.4 ± 0.1	2.9 ± 0.3	3.4 ± 0.2
CSDP	PIG	0.8 ± 0.1	1.3 ± 0.1	1.9 ± 0.1	2.8 ± 0.3	4.0 ± 0.3
	Gli	0.9 ± 0.1	1.1 ± 0.1	1.1 ± 0.2	1.5 ± 0.2	1.8 ± 0.2
CSDP + CBDP	PIG	0.9 ± 0.1	1.5 ± 0.1	3.5 ± 0.2	6.1 ± 0.3	7.0 ± 0.6
	Gli	1.1 ± 0.1	1.0 ± 0.1	1.2 ± 0.1	2.5 ± 0.2	3.2 ± 0.4

[a] Isolated rat adipocytes were electroporated in the absence (control) or presence of 100 μM CSDP without or with 300 μM CBDP, subsequently incubated (20 min, 37 °C) with increasing concentrations of PIG 41 (PIG) or glimepiride (Gli), and then assayed for 2-deoxyglucose transport. Quantitative evaluations of three different adipocyte incubations with measurements in duplicate each (mean ± SD) are given as fold stimulation of glucose transport above basal which was set at 1 for adipocytes electroporated in the absence of CSDP/CBDP.

Table 3: Increase of pp59^{Lyn} and pp125^{Fak} Activities and Caveolin Tyrosine Phosphorylation in Response to Glimepiride[a]

glimepiride [μM]	−	0.1 μM	0.3 μM	1 μM	3 μM	10 μM
pp59^{Lyn}	1 ± 0.1	1.2 ± 0.1	1.6 ± 0.2	2.9 ± 0.2	4.5 ± 0.6	4.9 ± 0.4
pp125^{Fak}	1 ± 0.2	0.9 ± 0.1	1.3 ± 0.1	1.8 ± 0.2	2.7 ± 0.4	3.6 ± 0.3
caveolin	1 ± 0.2	0.9 ± 0.1	1.4 ± 0.2	2.3 ± 0.2	2.8 ± 0.3	3.1 ± 0.4

[a] Isolated rat adipocytes were incubated (20 min, 37 °C) with increasing concentrations of glimepiride. pp59^{Lyn} and pp125^{Fak} activities were determined from total solubilized plasma membranes by immune complex kinase assay using [^{32}P]ATP and recombinant human IRS-1 and rabbit muscle enolase, respectively, as substrates. Caveolin tyrosine phosphorylation was measured by immunoprecipitation of caveolin-1 and subsequent immunoblotting for anti-phosphotyrosine using chemiluminescent detection. The amount of ^{32}P-labeled IRS-1 or enolase and tyrosine-phosphorylated caveolin obtained with pp59^{Lyn}, pp125^{Fak}, and caveolin from basal cells was set at 1. Quantitative evaluations of three different adipocyte incubations with measurements in triplicate each (mean ± SD) are given.

immunoprecipitation (Figures 8 and 10). The same experimental design demonstrated that PIG 41 also triggers the redistribution of pp59^{Lyn}, Gce1, and another adipocyte GPI protein, Nuc, from DIGs in concentration-dependent fashion (Figure 11, panels A and B). Interestingly, during sucrose gradient centrifugation, the redistributed proteins were recovered from fractions 10−14 exhibiting considerably higher buoyant density than typical DIGs (fractions 4−7). This material, called non-DIGs areas in the following, is characterized by a significantly lower caveolin content compared to DIGs, which was not affected by PIG treatment (Figure 11B), and a polypeptide composition different from both DIGs and total plasma membranes of rat adipocytes (G.M., C.J., S.W., W.F., manuscript in preparation). Since non-DIGs areas are derived from detergent-insoluble (1% TX-100 at 4 °C for 1 h) plasma membrane complexes (as is the case for DIGs), rat adipocytes apparently harbor two distinct species of raft domains differing in their constituent proteins and presumably cholesterol content (non-DIGs areas < DIGs). A subset of DIGs components exemplified by the GPI proteins, Gce1 and Nuc, and the NRTK pp59^{Lyn} became efficiently redistributed (up to 60−85%) from DIGs to non-DIGs areas in response to PIG 41 (Figure 11, panels A and B) and glimepiride (Figure 11C) but escaped distribution over the total plasma membrane.

Finally, we studied the involvement of CIR in the PIG- and glimepiride-induced redistribution of components from DIGs to non-DIGs areas (Figure 11). In control cells harboring active CIR, PIG 41 and glimepiride triggered a dramatic enrichment of Gce1, Nuc and pp59^{Lyn} in non-DIGs areas (8−18-fold and 3−6-fold, respectively, with resident caveolin used for normalization) accompanied by corresponding pronounced deprivement in DIGs (5−10-fold and 2−3-fold, respectively; Figure 11C). Upon inactivation of CIR with either trypsin *plus* NaCl or NEM, the amounts of Gce1, Nuc, and pp59^{Lyn} decreased 1.6−5-fold in DIGs and increased 3−8-fold in non-DIGs areas in the absence of any stimulus. Treatment of adipocytes harboring inactive CIR with PIG 41 did not significantly affect the elevated portion of these proteins in DIGs vs non-DIGs areas. In contrast, glimepiride induced a further 2−5-fold loss of Gce1, Nuc, and pp59^{Lyn} from DIGs and a concomitant 2−3-fold gain at non-DIGs areas (Figure 11). The apparent additive effects of glimepiride and inactivation of CIR on the redistribution of these proteins argue for the engagement of distinct mechanisms by the two stimuli. In reconstituted adipocytes, the distribution of Gce1, Nuc, and pp59^{Lyn} between DIGs and non-DIGs areas was similar to that of control cells with regard to both their low/high abundance in non-DIGs areas/DIGs in the basal state and vice versa high/low abundance in non-DIGs areas/DIGs in the PIG 41- and glimepiride-stimulated cells (Figure 11). These data strongly argue for a role of CIR in retention of a subset of components at DIGs in basal adipocytes as well as in their redistribution from DIGs to non-DIGs areas of the adipocyte plasma membrane in response to PIG but not glimepiride.

DISCUSSION

Biochemical and Pharmacological Stimuli for Release of Signaling Molecules from DIGs/Caveolin and Insulin-Mimetic Signaling/Action. The present study together with previously published data (*37*) reveals five different biochemical or pharmacological stimuli for triggering the redistribution of signaling proteins, such as NRTK and GPI proteins, from DIGs in isolated rat adipocytes. Independent of the type of stimulus, the redistribution leads to insulin-mimetic signaling via specific tyrosine phosphorylation processes to the glucose transport system. Treatment of intact cells with (i) trypsin and subsequently NaCl (Figure 7) or (ii) NEM (Figure 7), short-term incubation of intact cells with (iii) PIG (Figure 7, ref *37*) or (iv) the blood glucose-lowering third generation sulfonylurea glimepiride (Figures 8-11) or (v) introduction of CBDP derived from pp59^{Lyn} into intact cells (*37*) significantly reduces the amount of the GPI proteins, Gce1 and Nuc, and of the NRTK, pp125^{Fak} and pp59^{Lyn} residing in DIGs as well as the direct interaction of

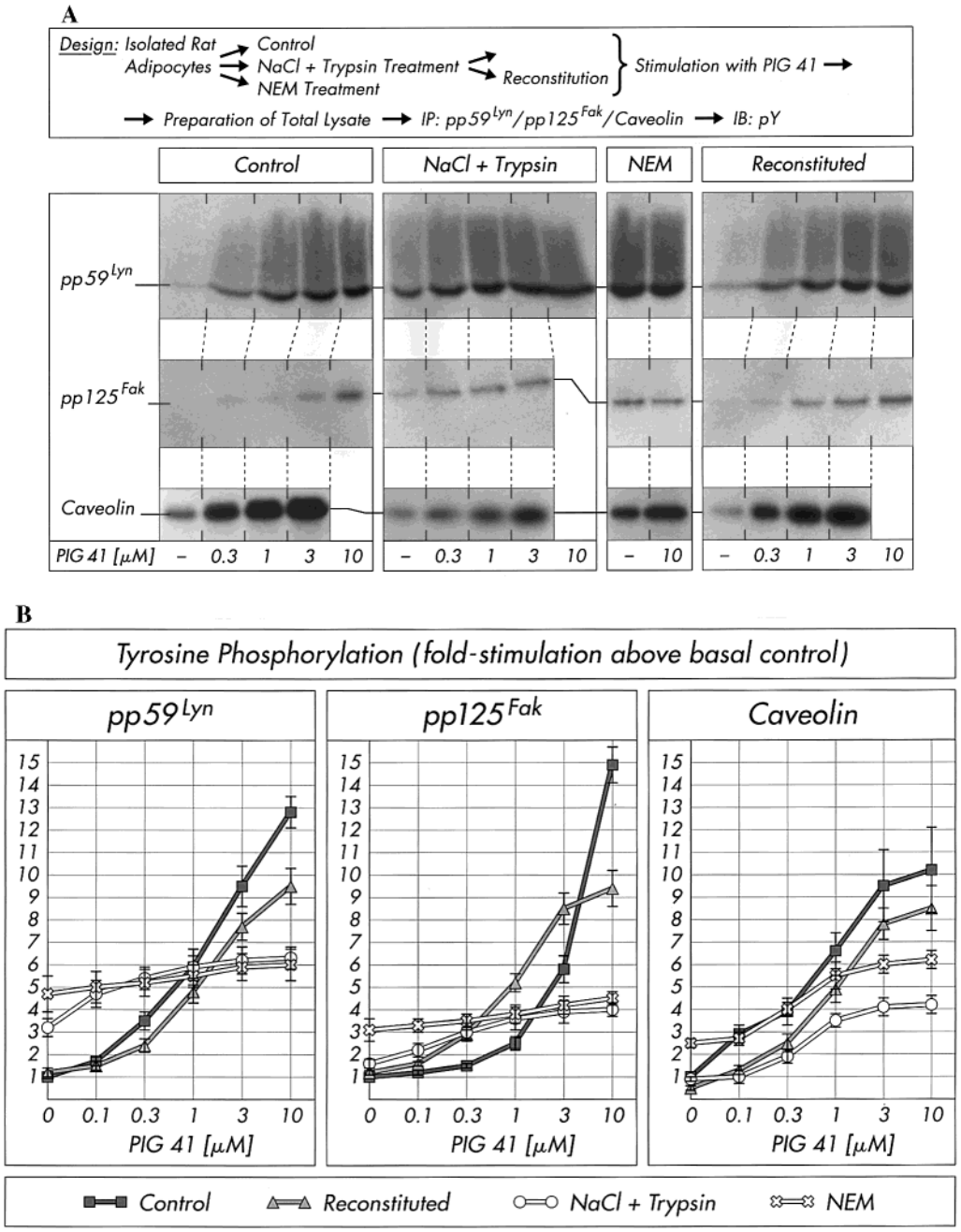

FIGURE 6: Inactivation of CIR induces PIG-independent tyrosine phosphorylation of pp59^{Lyn} and pp125^{Fak}. Isolated rat adipocytes were incubated in the absence (Control) or presence of trypsin *plus* NaCl or NEM. Portion of the trypsin/NaCl-treated adipocytes was subjected to reconstitution with trypsin/NaCl-extract. The four portions of adipocytes were incubated (20 min, 37 °C) in the absence or presence of increasing concentrations of PIG 41. pp59^{Lyn}, pp125^{Fak}, and caveolin were immunoprecipitated (IP) and then probed for phosphotyrosine (pY) by immunoblotting (IB) using chemiluminescent detection. (A) Chemiluminescent images of a typical experiment are shown repeated four times with similar results. (B) Quantitative evaluations of five different adipocyte incubations with measurements in triplicate each are given as fold stimulation (mean ± SD) with basal values (absence of PIG 41) for the control cells set at 1 in each case.

pp59^{Lyn} with caveolin in DIGs. The release/translocation from caveolin/DIGs of the signaling proteins elicited by stimuli I−IV correlates well to increased tyrosine phosphorylation and activity of pp59^{Lyn} and pp125^{Fak} (for points i and ii, see Figure 6; for point iii, see ref *37*; for point iv, see Table 3). Tyrosine phosphorylation and activation of pp125^{Fak} and pp59^{Lyn} is accompanied by elevated tyrosine phosphorylation of IRS-1/2 (for points i and ii, see Figures 4 and 5; for point iii, see Figures 3 and 4; for point iv, see Figures 2, 3, and 8). The induction of these tyrosine phosphorylation processes is in parallel to stimulation of glucose transport (for points i−iv, see Figure 1 and Table 1).

For glimepiride, we show here for the first time the induction of tyrosine phosphorylation of IRS-1 and IRS-2, association of PI-3K with IRS-1/2, and serine phosphorylation of PKB in a typical insulin target cell, the isolated adipocyte (Figure 2). From activated PI-3K and PKB, the signal may diverge to the various terminal effector systems which would explain the reported pleiotropic effects of glimepiride on both glucose and lipid metabolism in adipose and muscle cells in vitro (*59*) in the absence of a direct effect on the phosphorylation state of IRβ (Figure 2). This confirms earlier findings by Kobayashi and co-workers that glimepiride does not significantly alter the autophosphorylation

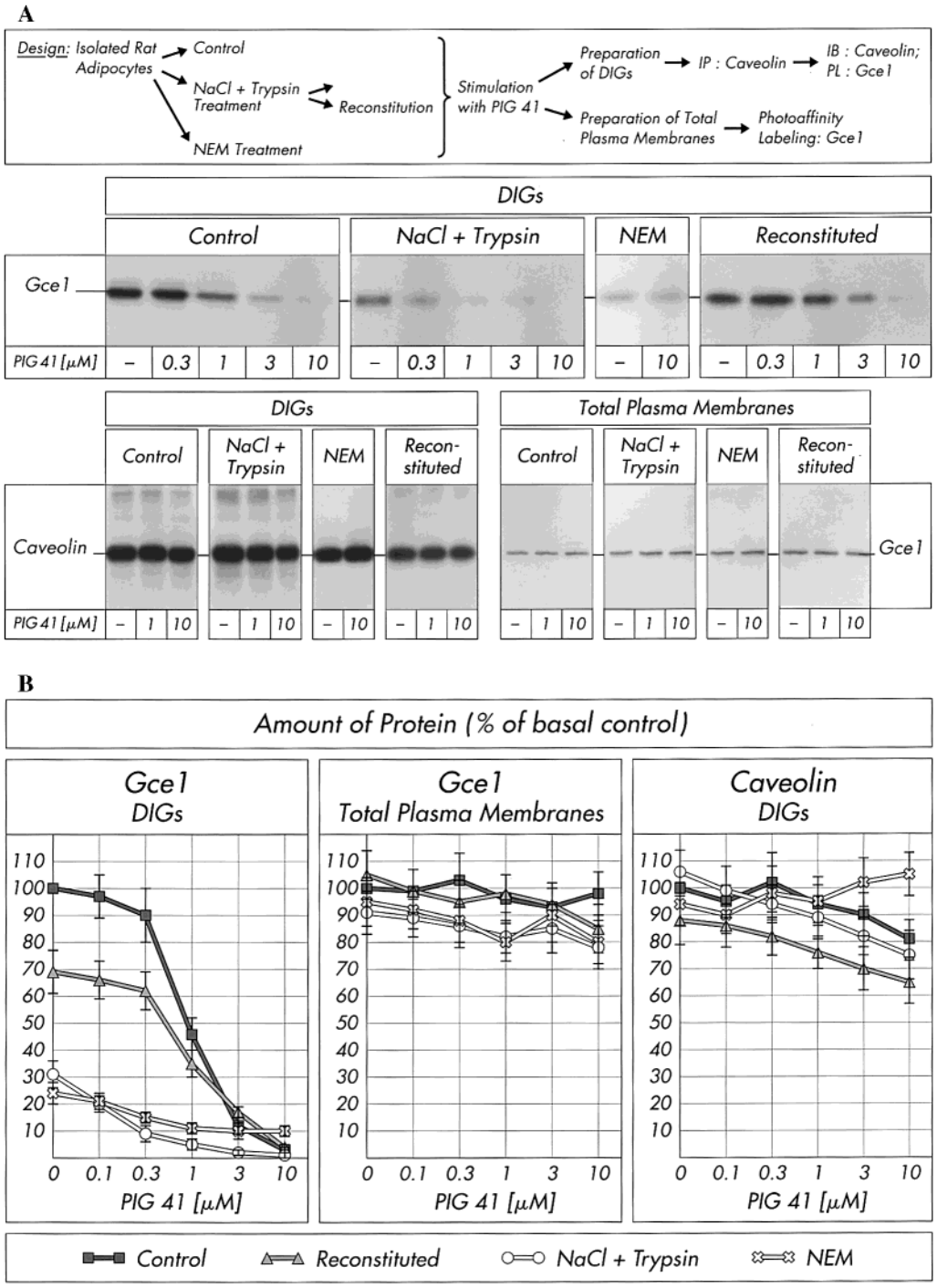

FIGURE 7: CIR is required for PIG-induced redistribution of Gce1 from DIGs. Isolated rat adipocytes were incubated in the absence (Control) or presence of trypsin *plus* NaCl or NEM. Portion of the trypsin/NaCl-treated adipocytes was subjected to reconstitution with trypsin/NaCl-extract. The four portions of adipocytes were incubated (20 min, 37 °C) in the absence or presence of increasing concentrations of PIG 41. Plasma membranes and DIGs from total cells (carbonate method) were prepared, suspended (nondissociating conditions), and used for photoaffinity labeling (PL) of Gce1 with 8-N_3-[^{32}P]cAMP (based on its cAMP-binding characteristics) or immunoprecipitation (IP) of caveolin. The immunoprecipitates were probed for caveolin by homologous immunoblotting (IB) using chemiluminescent detection or for Gce1 by photoaffinity labeling. (A) Phosphor/chemiluminescent images of a typical experiment are shown repeated three times with similar results. (B) Quantitative evaluations of four different adipocyte incubations with measurements in duplicate each are given as a percentage of basal values (absence of PIG 41) for control cells (mean ± SD) set at 100% in each case.

of the human insulin receptor heterologously expressed in rat fibroblasts (*41*). Taken together, these findings strongly suggest a causal relationship between the localization in DIGs/interaction with caveolin and low signaling activity of Gce1, pp125^{Fak}, and pp59^{Lyn} and vice versa between their redistribution/release from DIGs/caveolin and high signaling activity. Since introduction of excess CSDP into adipocytes efficiently blocks tyrosine phosphorylation and activation of pp59^{Lyn}, tyrosine phosphorylation of IRS-1/2, and glucose transport activation in response to both PIG (*37*) and glimepiride (Figure 5, Table 2), weakening of the interaction between caveolin and pp59^{Lyn} and concomitant movement

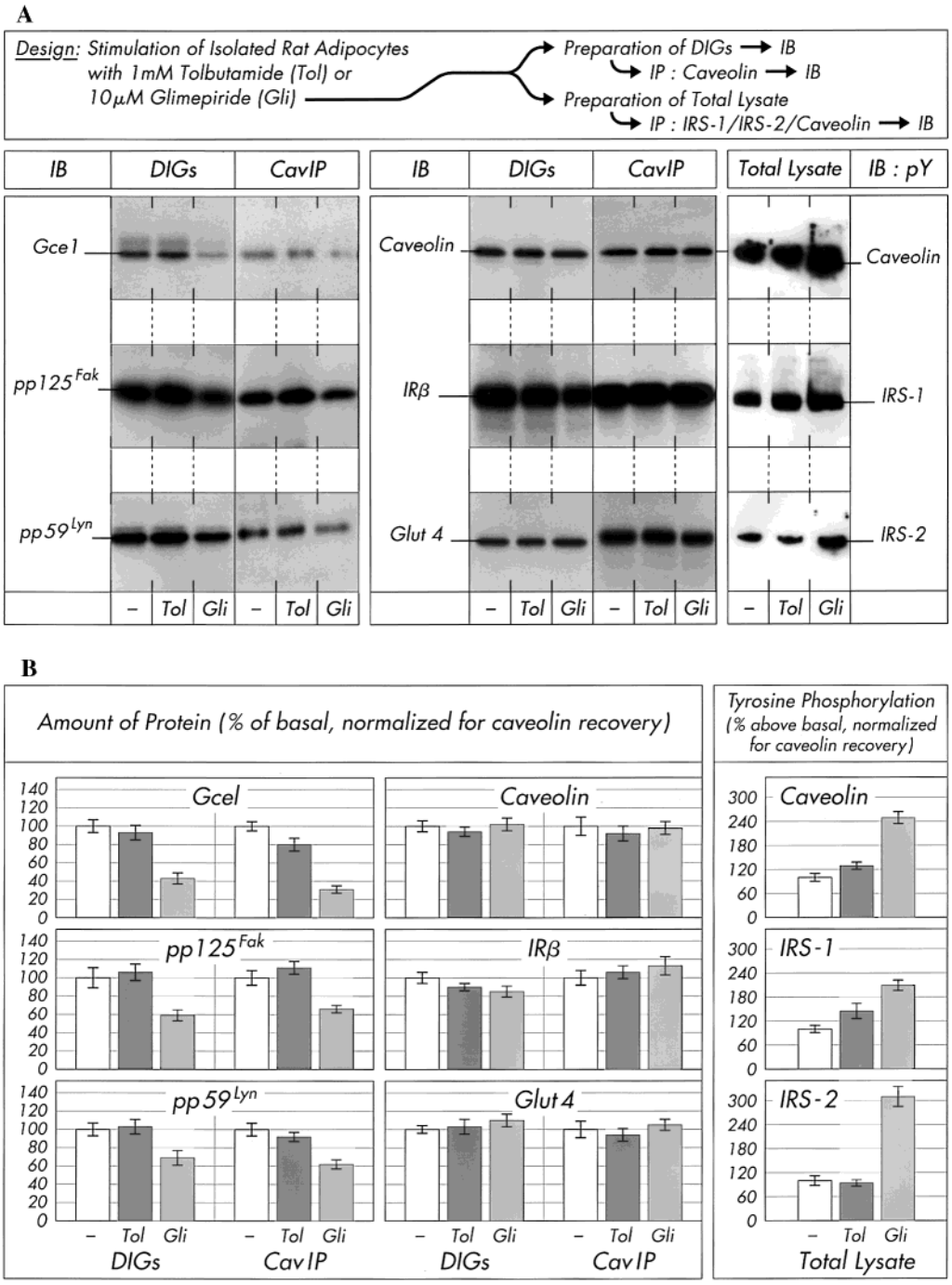

FIGURE 8: Sulfonylurea-induced redistribution of Gce1, pp125^{Fak}, and pp59^{Lyn} is correlated to tyrosine phosphorylation of caveolin and IRS-1/2. Isolated rat adipocytes were incubated (4 h, 37 °C) with 1 mM tolbutamide (Tol) or 10 μM glimepiride (Gli). DIGs (detergent method) or total cell lysates were prepared for immunoprecipitation (IP) of caveolin and IRS-1/2. The caveolin immunoprecipitates from DIGs (CavIP) and portions of the suspended DIGs (nondissociating conditions) were then assessed for the presence of Gce1 by photoaffinity labeling with 8-N_3-[^{32}P]cAMP or of pp125^{Fak}, pp59^{Lyn}, caveolin, IRβ and Glut4 by immunoblotting (IB) using chemiluminescent detection. The caveolin and IRS-1/2 immunoprecipitates from total lysates were immunoblotted for phosphotyrosine (pY) using chemiluminescent detection. (A) Phosphor/chemiluminescent images of a typical experiment are shown repeated three times with similar results. (B) Quantitative evaluations of four different adipocyte incubations with measurements in quadruplicate each are given as a percentage of basal values (set at 100% in the absence of sulfonylurea in each case, mean ± SD) after normalization for caveolin recovery (determined by homologous immunoblotting).

out from DIGs seems to be required or may even be sufficient for potent insulin-mimetic signaling and metabolic action. It remains to be elucidated whether the DIGs-caveolin-pp59^{Lyn} pathway is directly coupled to both the PI-3K-dependent and independent pathways which are necessary for glucose transport stimulation by insulin (see the introductory portion of this paper). Alternatively, activation of the PI-3K-independent pathway by PIG and glimepiride may be based on additional mechanisms distinct from redistribution and the DIGs-caveolin-pp59^{Lyn} pathway.

Localization of and Signaling via GPI Proteins. The DIGs-caveolin-pp59^{Lyn} pathway in adipocytes characterized in the present study and previous data on antibody cross-linking of GPI proteins in T cells (*63*−*66*) suggest the operation of

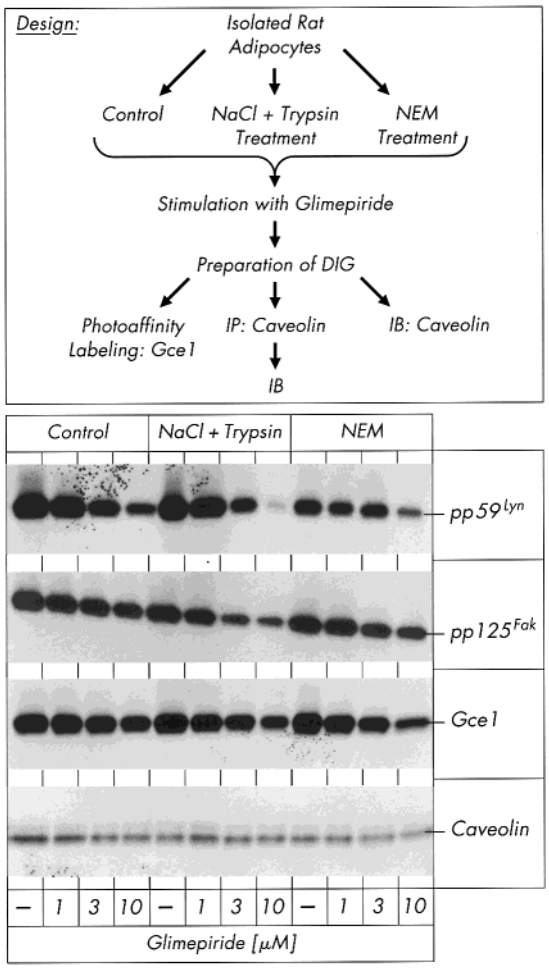

FIGURE 9: CIR is not required for glimepiride-induced redistribution of DIGs components. Isolated rat adipocytes were incubated in the absence (Control) or presence of trypsin *plus* NaCl or NEM. The three portions of adipocytes were incubated (20 min, 37 °C) in the absence or presence of increasing concentrations of glimepiride. DIGs from total cell lysates (carbonate method) were prepared and used for photoaffinity labeling of Gce1 with 8-N_3-[^{32}P]cAMP, direct immunoblotting (IB) for caveolin or immunoprecipitation (IP) of caveolin (dissociating conditions for analysis of pp59^{Lyn}; nondissociating conditions for analysis of pp125^{Fak}). The immunoprecipitates were assessed for the presence of pp59^{Lyn} and pp125^{Fak} by immunoblotting using chemiluminescent detection. Phosphor/chemiluminescent images are shown repeated three times with similar results.

(at least) two different modes for transmembrane signal transduction via GPI proteins using apparently mutually exclusive molecular mechanisms depending on the cell type (insulin-responsive vs hematopoetic) and the type of signaling (metabolic vs proliferative): (i) release of GPI proteins from DIGs and (ii) clustering of GPI proteins within DIGs. It is important to stress that both PIG 41 and glimepiride trigger the redistribution of two typical GPI proteins, Gce1 and Nuc, and of the dually acylated NRTK, pp59^{Lyn}, from DIGs to non-DIGs areas but not to the bulk detergent-soluble plasma membranes of adipocytes. The effect of both stimuli on the localization of other GPI proteins and acylated proteins and its tissue specificity remains to be studied as well as the biochemical/morphological nature and physiological relevance of non-DIGs areas. Nevertheless, the observed residence of Gce1 and Nuc with detergent-insoluble raft domains being either DIGs of low buoyant density or non-DIGs areas of higher buoyant density is compatible with the current view that essentially all GPI proteins can be recovered from detergent-insoluble plasma membrane domains (*17*, *25*, *67*). In fact, several purified GPI proteins and dually acylated signaling proteins (e.g., heterotrimeric G proteins) incorporated into DIGs-containing liposomes have been shown to form detergent-insoluble raft complexes without the requirement for binding to any other proteins (*68*−*70*). This reconstitution was found to critically depend on the presence of cholesterol in the phospholipid mixture and of long saturated fatty acids in the GPI moieties.

The available data are most easily reconciled with the assumption of general accumulation of GPI proteins as well as of dually acylated signaling proteins, such as the NRTK pp59^{Lyn}, at detergent-insoluble cholesterol-rich plasma membrane raft domains relying solely on the physical characteristics of their saturated acyl side chains (*63*−*70*). However, the fine-tuning of their distribution between DIGs and non-DIGs areas involves additional protein-mediated and regulatory mechanisms. For GPI proteins, a wide variability in the strength of their association with DIGs of low buoyant density has been reported (*71*, *72*), which may in fact reflect their differential intrinsic partitioning behavior between those and the detergent-insoluble non-DIGs areas of higher buoyant density. It remains to be studied whether the partitioning of GPI proteins other than Gce1 and Nuc is also modulated by PIG and glimepiride.

The present studies have elucidated the involvement of CIR in retention of Gce1, pp59^{Lyn} and pp125^{Fak} at DIGs under the negative control of PIG based on the following results. After trypsin/salt or NEM treatment of intact adipocytes, we observed considerable release of pp59^{Lyn} (Figure 11) and Gce1 (Figures 7 and 11) from DIGs/caveolin and DIGs, respectively, already in the basal state (absence of PIG) which can be further stimulated by PIG to a very moderate degree, only (Figures 7 and 11). This increased basal (but impaired PIG-induced) redistribution after inactivation of CIR is correlated well to elevated basal (but reduced PIG-stimulated) tyrosine phosphorylation of pp59^{Lyn}, pp125^{Fak} (Figure 6), and IRS-1/2 (Figure 4) as well as glucose transport activation (Figure 1). After reconstitution of the pretreated adipocytes with extract containing active CIR, both the low basal activities and the high responsiveness toward PIG is restored to about the level observed in mock-treated cells. This is correlated well to the regained association of Gce1, pp59^{Lyn}, and pp125^{Fak} with DIGs and of pp59^{Lyn} with caveolin in the basal state as well as to their regained ability of being released in response to PIG (Figures 7 and 11). These findings are compatible with involvement of CIR in keeping certain signaling components (e.g., pp59^{Lyn}) in the basal inactive state (by recruitment to caveolin-containing DIGs).

Mechanism of PIG-Induced Redistribution of GPI Proteins. CIR is presumably identical with p115 which is released from the adipocyte surface by trypsin/salt treatment and labeled by [^{14}C]NEM treatment of intact adipocytes (*46*). The molecular mode of CIR action on the localization of GPI proteins remains unclear, but the following explanations can be envisioned. Since PIG structures represent the conserved polar core glycan headgroup of the GPI anchor of GPI proteins (*31*, *32*), it is reasonable to suggest that the DIGs resident CIR recognizes the PIG moiety within intact GPI protein anchors thereby recruiting GPI proteins to DIGs.

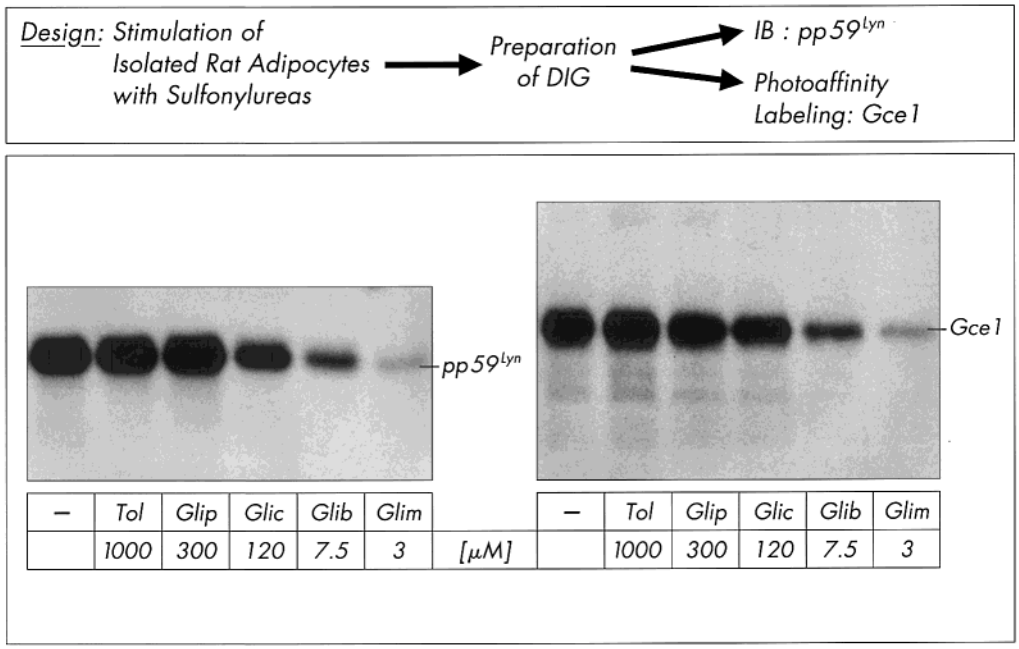

FIGURE 10: Different sulfonylureas trigger redistribution of Gce1 and pp59^{Lyn} from DIGs with different efficiency. Isolated rat adipocytes were incubated (20 min, 37 °C) with glimepiride (Glim), glibenclamide (Glib), tolbutamide (Tol), glipizide (Glip), or gliclazide (Glic) at the concentrations indicated. DIGs were prepared from total cell lysates (detergent method), suspended (dissociating conditions), and then probed for the presence of Gce1 by photoaffinity labeling with 8-N_3-[^{32}P]cAMP and of pp59^{Lyn} by immunoblotting using chemiluminescent detection. The figure shows phosphor/chemiluminescent images repeated two times with similar results.

Preliminary binding experiments using radiolabeled PIG derivatives or BiaCore interaction analysis indicate that CIR partially purified from octylglucoside-solubilized adipocyte DIGs interacts with high affinity and specificity with PIG 41 (but not PIG 1), arguing for a role of CIR as PIG receptor in adipocytes (M. Gerl, M. Quint and G.M., unpublished data). Consequently, active PIG added to the incubation medium of intact adipocytes would cause concentration-dependent competitive displacement of GPI proteins from CIR resulting in movement from DIGs to non-DIGs areas of those GPI proteins, at least, with low inherent affinity for DIGs, representatives of which may be Gce1 and Nuc. Alternatively, the higher cholesterol content of DIGs vs non-DIGs areas may be sufficient for enrichment of GPI proteins at DIGs, and this DIGs-targeting function of cholesterol may be masked by CIR upon treatment of adipocytes with PIG, trypsin *plus* NaCl or NEM through direct sequestration of cholesterol or some other means. We are currently investigating the effect of cholesterol depletion of the adipocyte plasma membrane on (PIG-regulated and CIR-dependent) GPI protein distribution.

Mechanism of PIG-Induced Redistribution of NRTK. The partitioning of NRTK and other acylated signaling proteins between DIGs and non-DIGs areas within detergent-insoluble raft domains may be determined by interaction of their CBD with the CSD shifting the equilibrium toward DIGs. Consequently, competitive displacement of this interaction by excess of CBD will result in movement of pp59^{Lyn} from DIGs to non-DIGs areas. However, it is difficult to understand how PIG via GPI proteins manage to disrupt the association of NRTK with caveolin and DIGs given the fact that GPI proteins are restricted to the outer leaflet of the membrane bilayer and cannot interact with inner leaflet proteins (including caveolin). Part of the proposed DIGs-targeting function of cholesterol may rely on increasing the efficiacy of the CSD−CBD interaction. Consequently, masking of cholesterol by PIG-activated CIR will lead to release of CBD-containing proteins from DIGs to non-DIGs areas. Alternatively, CIR may operate as the postulated transmembrane linker protein by direct simultaneous binding to the GPI anchor of GPI proteins and the protein moiety and/or acyl chains of NRTK (*73*) and this linker function may be subjected to regulation by PIG. Furthermore, it cannot be excluded that the PIG-induced redistribution of GPI proteins may somehow interfere with the tight and parallel packing of the long saturated fatty acyl chains of GPI proteins (*16*, *17*, *74*) and NRTK simultaneously at the outer and inner leaflets within DIGs, respectively. It is conceivable that the apparent loss of saturated GPI protein-bound fatty acids at the outer leaflet may result in passive diffusion of saturated NRTK-bound fatty acids at the inner leaflet from DIGs to non-DIGs areas. Future studies have to address the molecular link between the release of GPI proteins from DIGs and the dissociation of NRTK from DIGs and caveolin as well as the causal relationship between release of NRTK from DIGs and caveolin.

Mechanism of Glimepiride-Induced Redistribution of Signaling Proteins. In contrast to PIG, sulfonylureas trigger redistribution independent of CIR provided they manage to interact with GPI lipids. Glimepiride has been demonstrated to intercalate into DIGs of the adipocyte plasma membrane in a time-dependent and nonsaturable fashion. This is based on direct interaction with two distinct GPI lipid species (identified by photoaffinity labeling) rather than on high-affinity binding to a receptor protein (*44*), such as one of the sulfonylurea receptors in case of pancreatic β-cells (*75*, *76*) or CIR in case of PIG and adipose cells (see above). The accumulation of glimepiride at DIGs vs non-DIGs areas seems to rely in part on its pronounced lipophilicity. In contrast, the second and first generation sulfonylureas,

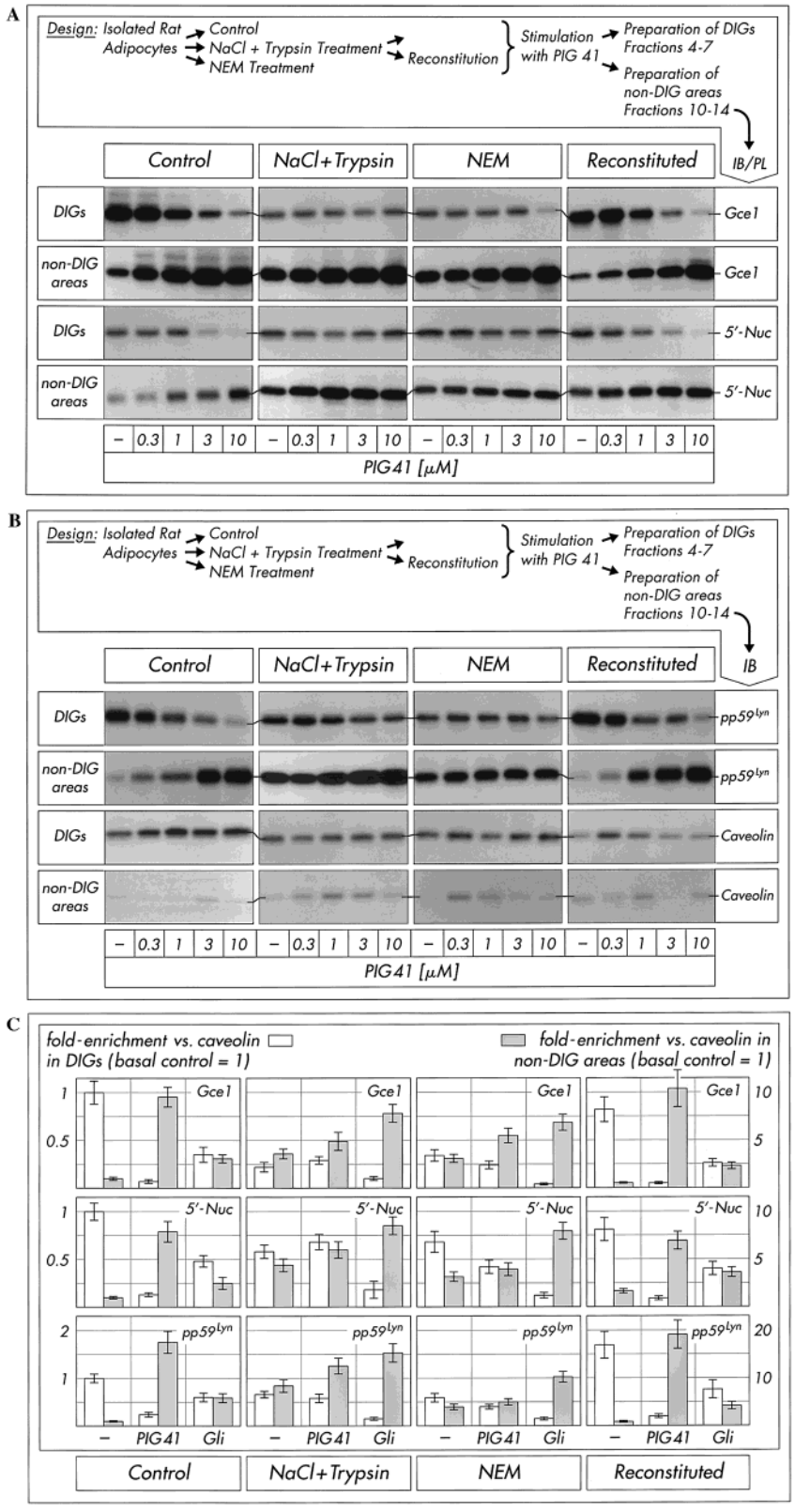

FIGURE 11: PIG- or glimepiride-induced redistribution of Gce1, Nuc, and pp59^{Lyn} is based on their movement from DIGs to detergent-insoluble non-DIGs areas of the plasma membrane. Isolated rat adipocytes were incubated in the absence (Control) or presence of trypsin *plus* NaCl or NEM. Portion of the trypsin/NaCl-treated adipocytes was subjected to reconstitution with trypsin/NaCl-extract. The four portions of adipocytes were incubated (20 min, 37 °C) in the absence or presence of increasing concentrations of PIG 41 (A, B) or 3 μM PIG 41 and glimepiride (C). From total plasma membranes DIGs and non-DIGs areas were prepared (carbonate method), suspended (dissociating conditions) and used for photoaffinity labeling (PL) of Gce1 with 8-N_3-[^{32}P]cAMP or immunoblotting (IB) of Nuc, pp59^{Lyn} and caveolin using chemiluminescent detection. (A, B) Phosphor/chemiluminescent images of a typical experiment are shown repeated two times with similar results. (C) Quantitative evaluations of three different adipocyte incubations for each treatment (absence or presence of 3 μM PIG 41 or 3 μM glimepiride) with measurements in quadruplicate each are given as fold-enrichment (mean ± SD) of each protein vs caveolin which was used for normalization of each treatment. Basal values (absence of PIG 41 or glimepiride) for control cells were set at 1 for DIGs (open bars, left abscissa) and non-DIGs areas (closed bars, right abscissa), respectively, for each protein.

glibenclamide and tolbutamide, characterized by medium and low lipophilicity, respectively, were found to be photocross-linked to GPI lipids, to induce redistribution of Gce1, $pp125^{Fak}$, and $pp59^{Lyn}$, to stimulate tyrosine phosphorylation of IRS-1/2 and to activate glucose transport to moderate and very low level, respectively, compared to glimepiride (Figures 8 and 10; see refs *44* and *59*). Thus, glimepiride and to a limited degree glibenclamide (and other second generation sulfonylureas), but hardly tolbutamide, may physically interfere with the structural organization of adipocyte DIGs by direct intercalation thereby triggering release of signaling molecules from DIGs. As an alternative to a certain threshold of lipophilicity as requirement for intercalation into the lipid core, sulfonylureas may directly bind to the glycan headgroups of the GPI anchor. Either of the two properties may elicit physical interference with the highly ordered DIGs structure, which leads to weakening of the tight parallel packing of the saturated acyl chains within the lipid core of DIGs. The consequences on the partitioning of GPI proteins between DIGs and non-DIGs areas may be similar to the putative CIR-mediated masking of cholesterol function in response to PIG. However, despite unraveling of a clear-cut positive correlation between the insulinindependent blood glucose-lowering activity and potency in the redistribution of signaling proteins exhibited by structurally different sulfonylureas of the first, second, and third generation (see Figure 10), no unambigious structure−activity relationship could be delineated so far for interference with the function/structure of DIGs as well as activation of the DIGs-caveolin-$pp59^{Lyn}$-IRS pathway.

The functional role of tyrosine phosphorylation of caveolin in rat adipocytes in response to PIG 41 (Figure 6) and glimepiride (but not tolbutamide) (Figure 8) remains unclear. It may facilitate the dissociation of caveolin from $pp59^{Lyn}$ and other DIGs components and/or stabilize their disassembled state. $pp59^{Lyn}$ may function as caveolin kinase in PIG-treated adipocytes since other Src family protooncogenes, such as c-Src and Fyn, have been reported to be responsible for tyrosine phosphorylation of caveolin-1 in transformed cells (*12*, *60*, *61*). In cultured endothelial cells, oxidative stress and tyrosine phosphatase inhibitors caused phosphorylation of caveolin at tyrosine-14 accompanied by internalization of caveolae (*62*). This raised the intriguing possibility that dissociation of caveolin from DIGs components is promoted/regulated by endocytosis of caveolae harboring caveolin but leaving back at the plasma membrane DIGs lacking caveolin but harboring GPI proteins and derepressed $pp59^{Lyn}$ which would constitute a positive feedback loop. It is tempting to speculate that internalization of vesicles enriched in caveolin with bound cholesterol but deprived of other DIGs components will result in conversion of DIGs into non-DIGs areas. These finally represent the location of GPI proteins and NRTK as observed after PIG and glimepiride stimulation of adipocytes. The mechanism of DIGs-to-non-DIGs areas conversion represents an alternative to the active movement of components from DIGs to non-DIGs areas. In addition, tyrosine-phosphorylated caveolin may act as an adaptor protein from which (insulin-mimetic) signaling to an as yet unknown (metabolic) pathway is initiated.

It is amazing that lipophilic sulfonylurea drugs and polar PIG may induce the same structural/functional alterations in DIGs by completely different molecular mechanisms, direct partitioning into DIGs and binding to CIR/p115, respectively. Interestingly, preliminary data argue for a considerable upregulation of flottilin and/or caveolin gene expression in skeletal muscle of insulin-resistant animals (stroke-prone spontaneously hypertensive rats) and humans (polycystic overian syndrome) (*77*). Thus, pharmacological suppression of the inhibitory role of caveolin/flottilin on insulin signaling (via the Cbl pathway) or insulin-mimetic signaling (via the DIGs-caveolin-$pp59^{Lyn}$ pathway) in insulin target cells may be helpful for the therapy of insulin resistance, the hallmark of type II diabetes mellitus.

REFERENCES

1. Gustafson, T. A., Moodie, S. A., and Lavan, B. E. (1998) *Rev. Physiol. Biochem. Pharmacol. 137*, 1−192.
2. Czech, M. P., and Corvera, S. (1999) *J. Biol. Chem. 274*, 1865−1868.
3. Nystrom, F. H., and Quon, M. J. (1999) *Cell. Signalling 11*, 563−574.
4. Cohen, P., Alessi, D. R., and Cross, D. A. (1997) *FEBS Lett. 410*, 3−10.
5. Shepherd, P. R., Withers, D. J., and Siddle, K. (1998) *Biochem. J. 333*, 471−490.
6. Pessin, J. E., Thurmond, D. C., Elmendorf, J. S., Coker, K. J., and Okada, S. (1999) *J. Biol. Chem. 274*, 2593−2596.
7. Jiang, T., Sweeney, G., Rudolf, M. T., Klip, A., Traynor-Kaplan, A., and Tsien, R. Y. (1998) *J. Biol. Chem. 273*, 11017−11024.
8. Krook, A., Whitehead, J. P., Dobson, S. P., Griffiths, M. R., Ouwens, M., Baker, C., Sen, S. K., Maassen, J. A., and Siddle K. (1997) *Proc. Natl. Acad. Sci. U.S.A. 94*, 30208−30214.
9. Wiese, R. J., Mastick, C. C., Lazar, D. F., and Saltiel, A. R. (1995) *J. Biol. Chem. 270*, 3442−3446.
10. Guilherme, A., and Czech, M. P. (1998) *J. Biol. Chem. 273*, 33119−33122.
11. White, M. F. (1998) *Mol. Cell. Biochem. 182*, 3−11.
12. Mastick, C. C., Brady, M. J., and Saltiel, A. R. (1995) *J. Cell Biol. 129*, 1523−1531.
13. Ribon, V., and Saltiel, A. R. (1997) *Biochem. J. 324*, 839−845.
14. Ribon, V., Printen, J. A., Hoffman, N. G., Kay, B. K., and Saltiel, A. R. (1998) *Mol. Cell. Biol. 18*, 872−879.
15. Baumann, C. A., Ribon, V., Kanzaki, M., Thurmond, D. C., Mora, S. Shigematsu, S., Bickel, P. E., Pessin, J. E., and Saltiel, A. R. (2000) *Nature 407*, 202−207.
16. Harder, T., Scheiffele, P., Verkade, P., and Simons, K. (1998) *J. Cell Biol. 141*, 929.
17. Brown, D. A., and London, E. (1998) *J. Membr. Biol. 164*, 103−114.
18. Anderson, R. G. W. (1998) *Annu. Rev. Biochem. 67*, 199−225.
19. Smart, E. J., Graf, G. A., McNiven, M. A., Sessa, W. C., Engelman, J. A., Scherer, P. E., Okamoto, T., and Lisanti, M. P. (1999) *Mol. Cell. Biol. 19*, 7289−7304.
20. Stauffer, T. P., and Meyer, T. (1997) *J. Cell Biol. 139*, 1447−1454.
21. Sheets, E. D., Lee, G. M., Simson, R., and Jacobson, K. (1997) *Biochemistry 36*, 12449−12458.
22. Lisanti, M. P., Scherer, P. E., Tang, Z. L., and Sargiacomo, M. (1994) *Trends Cell Biol. 4*, 231−235.
23. Schlegel, A., Volonte, D., and Engelmann, J. A. (1999) *Cell. Signalling 10*, 457−463.
24. Scherer, P. E., Lewis, R. Y., Volonte, D., Engelman, J. A., Galbiati, F., Couet, J., Kohtz, D. S., van Donselaar, E., Peters, P., and Lisanti, M. P. (1997) *J. Biol. Chem. 272*, 29337−29346.
25. Simons, K., and Ikonen, E. (1997) *Nature 387*, 569−572.
26. Glenney, J. R. (1992) *FEBS Lett. 314*, 45−48.
27. Das, K., Lewis, R. Y., Scherer, P. E., and Lisanti, M. P. (1999) *J. Biol. Chem. 274*, 18721−18726.

28. Okamoto, T., Schlegel, A., Scherer, P. E., and Scherer, M. P. (1998) *J. Biol. Chem. 273*, 5419−5422.
29. Ribon, V., Johnson, J. H., Camp, H. S., and Saltiel, A. R. (1998) *Proc. Natl. Acad. Sci. U.S.A. 95*, 14751−14756.
30. Bickel, P. E., Scherer, P. E., Schnitzer, J. E., Oh, P., Lisanti, M. P., and Lodish, H. F. (1997) *J. Biol. Chem. 272*, 13793−13802.
31. Müller, G., Wied, S., Crecelius, A., Kessler, A., and Eckel, J. (1997) *Endocrinology 138*, 3459−3475.
32. Frick, W., Bauer, A., Bauer, J., Wied, S., and Müller, G. (1998) *Biochemistry 37*, 13421−13436.
33. Müller, G., and Wied, S. (1993) *Diabetes 42*, 1852−1867.
34. Müller, G., Wied, S., Wetekam, E.-M., Crecelius, A., Unkelbach, A., and Pünter, J. (1994) *Biochem. Pharmacol. 48*, 985−996.
35. Frick, W., Bauer, A., Bauer, J., Wied, S., and Müller, G. (1998) *Biochem. J. 336*, 163−181.
36. Müller, G., Wied, S., and Frick, F. (2000) *Mol. Cell. Biol. 20*, 4708−4723.
37. Müller, G., Jung, C., Wied, S., Welte, S., Jordan, H., and Frick, W. (2001) *Mol. Cell. Biol. 21*, 4553−4567.
38. Lebovitz, H. E. (1990) in *Ellenberg and Rifkin's Diabetes Mellitus. Theory and Practise*. (Rifkin, H., and Porte, D., Eds.) pp 554−574, Elsevier press, New York.
39. Langtry, H. D., and Balfour, J. A. (1998) *Drugs 55*, 563−584.
40. Bähr, M., v. Holtey, M., Müller, G., and Eckel, J. (1995) *Endocrinology 136*, 2547−2553.
41. Takada, Y., Takata, Y., Iwanishi, M., Imamura, T., Sawa, T., Morioka, H., Ishihara, H., Ishiki, M., Usui, I., Temaru, R., Urakaze, M., Satoh, Y., Inami, T., Tsuda, S., and Kobayashi, M. (1996) *Eur. J. Pharmacol. 308*, 205−210.
42. Volk, A., Maerker, E., Rett, K., Häring, H.-U., and Overkamp, D. (2000) *Diabetologia 43* (Suppl. 1), A39 (abstr.).
43. Müller, G., Wied, S., and Welte, S. (2000) *Chem. Phys. Lipids 7*, 7−8 (abstr.).
44. Müller, G., and Geisen, K. (1996) *Horm. Metabol. Res. 28*, 469−487.
45. Müller, G., Ertl, J., Gerl, M., and Preibisch, G. (1997) *J. Biol. Chem. 272*, 10585−10593.
46. Müller, G., Wied, S., Piossek, C., Bauer, A., Bauer, J., and Frick, W. (1998) *Mol. Med. 4*, 299−323.
47. Müller, G., Wetekam, E.-A., Jung, C., and Bandlow, W. (1994) *Biochemistry 33*, 12149−12159.
48. Müller, G., Dearey, E.-A., Korndörfer, A., and Bandlow, W. (1994) *J. Cell Biol. 126*, 1267−1276.
49. Araki, E., Lipes, M. A., Patti, M. E., Brüning, J. C., Haag, B., Johnson, R. S., and Kahn, C. R. (1994) *Nature 372*, 186−190.
50. Tamemoto, H., Kadowaki, T., Tobe, K., Yagi, T., Sakura, H., Hayakawa, T., Terauchi, Y., Ueki, K., and Satoh, S. (1994) *Nature 372*, 182−186.
51. Withers, D. J., Gutierrez, J. S., Towery, H., Burks, D. J., Ren, J. M., Previs, S., Zhang, Y., Bernal, D., Pons, S., Shulman, G. I., Bonner-Weir, S., and White, M. F. (1998) *Nature 391*, 900−904.
52. Giovannone, B., Scaldaferri, M. L., Federici, M., Porzio, O., Lauro, D., Fusco, A., Sbraccia, P., Borboni, P., Lauro, R., and Sesti, G. (2000) *Diabetes Metabol. Res. Rev. 16*, 434−441.
53. Kido, Y., Burks, D. J., and Whiters, D. (2000) *J. Clin. Invest. 105*, 199−205.
54. Müller, G., and Frick, W. (1999) *Cell. Mol. Life Sci. 56*, 945−970.
55. Couet, J., Li, S., Okamoto, T., Ikezu, T., and Lisanti, M. P. (1997) *J. Biol. Chem. 272*, 6525−6533.
56. Couet, J., Sargiacomo, M., and Lisanti, M. P. (1997) *J. Biol. Chem. 272*, 30429−30438.
57. Li, S., Couet, J., and Lisanti, M. P. (1996) *J. Biol. Chem. 272*, 29182−29190.
58. Razani, B., Rubin, C. S., and Lisanti, M. P. (1999) *J. Biol. Chem. 274*, 26353−26360.
59. Müller, G. (2000) *Mol. Med. 6*, 907−933.
60. Li, S., Seitz, R., and Lisanti, M. P. (1996) *J. Biol. Chem. 271*, 3863−3868.
61. Glenney, J. R. (1989) *J. Biol. Chem. 264*, 20163−20166.
62. Aoki, T., Nomura, R., and Fujimoto, T. (1999) *Exp. Cell Res. 253*, 629−636.
63. Robinson, P. J., Millrain, M., Antoniou, J., Simpson, E., and Mellor, A. L. (1989) *Nature 342*, 85−87.
64. Su, B., Waneck, G. L., Flavell, R. A., and Bothwell, A. L. M. (1991) *J. Cell Biol. 112*, 377−384.
65. Shenoy-Scaria, A. M., Kwong, J., Fujita, T., Olszowy, M. W., Shaw, A. S., and Lublin, D. M. (1992) *J. Immunol. 149*, 3535−3541.
66. Van der Berg, C. W., Cinek, T., Hallett, M. B., Horejsi, V., and Morgan B. P. (1995) *J. Cell Biol. 131*, 669−677.
67. Shaul, P. W., and Anderson, R. G. (1998) *Am. J. Physiol. 275*, L843−L851.
68. Kihn, L., Rutkowski, D., and Stinson, R. (1990) *Biochem. Cell Biol. 68*, 1112−1118.
69. Schreier, H., Moran, P., and Caras, I. W. (1994) *J. Biol. Chem. 269*, 9090−9098.
70. Schroeder, R., London, E., and Brown, D. (1994) *Proc. Natl. Acad. Sci. U.S.A. 91*, 12130−12134.
71. Nosjean, O., Briolay, A., and Roux, B. (1997) *Biochim. Biophys. Acta 1331*, 153−186.
72. Vogel, M., Kowalewski, H., Zimmermann, H., Hooper, N. M., and Turner, A. J. (1992) *Biochem. J. 284*, 621−624.
73. Brown, D. (1993) *Curr. Opin. Immunol. 5*, 349−354.
74. Rietveld, A., and Simons, K. (1998) *Biochim. Biophys. Acta 1376*, 467−479.
75. Kramer. W., Müller, G., Girbig, F., Gutjahr, U., Kowalewski, S., Hartz, D., and Summ, H.-D. (1994) *Biochim. Biophys. Acta 1191*, 278−290.
76. Aguilar-Bryan, L., and Bryan, J. (1999) *Endocr. Rev. 20*, 101−135.
77. Cairns, F., James, D. J., Graham, D., Salt, I. P., Murphy, G. J., Dominiczak, A. F., Connell, J. M. C., and Gould, G. W. (2001) *Biochem. Soc. Trans. 29* (part 3), A70 (abstr.).

BI0108352